Biology of Reproduction, 2022, **106(4)**, 710–729
https://doi.org/10.1093/biolre/ioab243
Advance access publication date 28 December 2021
Research Article

Developing a reproducible protocol for culturing functional confluent monolayers of differentiated equine oviduct epithelial cells†

Bart Leemans[1,2], Elizabeth G. Bromfield[3,4], Tom A.E. Stout[2], Mabel Vos[2], Hanna Van Der Ham[2], Ramada Van Beek[2], Ann Van Soom[1], Bart M. Gadella[1,3,5,*] and Heiko Henning[5]

[1]Department of Reproduction, Obstetrics and Herd Health, Faculty of Veterinary Medicine, Ghent University, Ghent, Belgium
[2]Department of Clinical Sciences, Utrecht University, Utrecht, The Netherlands
[3]Biomolecular Health Sciences, Utrecht University, Utrecht, The Netherlands
[4]Priority Research Centre for Reproductive Science, Faculty of Science, University of Newcastle, Newcastle, Australia
[5]Population Health Sciences, Faculty of Veterinary Medicine, Utrecht University, Utrecht, The Netherlands
***Correspondence:** Yalelaan 7, 3584 CM Utrecht, The Netherlands. E-mail: b.m.gadella@uu.nl
†**Grant Support:** This study was supported by the Research Foundation – Flanders (FWO-Flanders; grant number 12I0517N) and EU COST Action 16119 CellFit.

Abstract

We describe the development of two methods for obtaining confluent monolayers of polarized, differentiated equine oviduct epithelial cells (EOEC) in Transwell inserts and microfluidic chips. EOECs from the ampulla were isolated post-mortem and seeded either (1) directly onto a microporous membrane as differentiated EOECs (direct seeding protocol) or (2) first cultured to a confluent de-differentiated monolayer in conventional wells, then trypsinized and seeded onto a microporous membrane (re-differentiation protocol). Maintenance or induction of EOEC differentiation in these systems was achieved by air–liquid interface introduction. Monolayers cultured via both protocols were characterized by columnar, cytokeratin 19-positive EOECs in Transwell inserts. However, only the re-differentiation protocol could be transferred successfully to the microfluidic chips. Integrity of the monolayers was confirmed by transepithelial resistance measurements, tracer flux, and the demonstration of an intimate network of tight junctions. Using the direct protocol, 28% of EOECs showed secondary cilia at the apical surface in a diffuse pattern. In contrast, re-differentiated polarized EOECs rarely showed secondary cilia in either culture system (>90% of the monolayers showed <1% ciliated EOECs). Occasionally (5–10%), re-differentiated monolayers with 11–27% EOECs with secondary cilia in a diffuse pattern were obtained. Additionally, nuclear progesterone receptor expression was found to be inhibited by simulated luteal phase hormone concentrations, and sperm binding to cilia was higher for re-differentiated EOEC monolayers exposed to estrogen–progesterone concentrations mimicking the follicular rather than luteal phase. Overall, a functional equine oviduct model was established with close morphological resemblance to in vivo oviduct epithelium.

Summary Sentence

A functional equine in vitro oviduct epithelium model was established in Transwell inserts and microfluidic chips using either a direct seeding or a de-differentiation/re-differentiation protocol.

Keywords: oviduct, equine, Transwell culture, cilia, primary cell culture, microfluidic chip

Introduction

To date, conventional equine in vitro fertilization (IVF) has been poorly successful, with only two foals reported [1, 2] Moreover, the protocol used to produce these foals has not proven to be repeatable, and conventional equine IVF remains poorly successful [1, 2, 3, 4, 5, 6, 7]. It is generally believed that stallion sperm fail to penetrate the zona pellucida in vitro either due to inadequate zona maturation or, more probably, poor activation/capacitation of spermatozoa [8, 9].

The lumen of the equine oviduct is an essential environment for equine gametes to achieve fertilization in vivo. Experimental evidence supporting the importance of the equine oviduct for enabling fertilization includes: (1) the fact that IVF using in vivo matured oocytes is not successful [1], whereas in vitro matured oocytes transferred to the oviduct of an inseminated mare yield similar pregnancy rates to artificial insemination prior to normal ovulation [3]. This indicates that in vitro matured oocytes are capable of being fertilized normally and do not require the in vivo follicular environment during maturation. (2) When spermatozoa are directly inseminated into the equine oviduct via the infundibulum, pregnancy rates are similar to those obtained after artificial insemination into the uterine body [10]. This suggests that passage through the uterus is not obligatory for stallion spermatozoa to be primed for capacitation/fertilization.

Generally, it is suggested that high rates of fertilization in vivo are permitted by a highly supportive, hormone-directed oviductal environment [11]. Each oviduct consists of an isthmus and ampulla, located at the uterine and ovarian ends, respectively. In both parts of the oviduct, the lumen is lined by

Received: March 18, 2021. **Revised:** July 14, 2021. **Accepted:** December 24, 2021

an epithelium with two major populations of highly polarized columnar cells, namely ciliated and secretory (non-ciliated) cells [12]. The ciliated cells play a role in gamete transport and sperm-binding and, in most species, predominate in the isthmus [13, 14]. The secretory cells, that predominate in the ampulla, produce oviductal fluid [15]. However, an inversed predominance of ciliated versus non-ciliated cells has been reported in the respective oviductal segments of the horse [16]. When spermatozoa arrive in the oviduct, they bind to oviduct epithelial cells (OECs) in the isthmus, an interaction that prolongs their lifespan. Sperm are stored in this "sperm reservoir" until the time is right to detach and undergo capacitation (maturation) in preparation for fertilization [15]. Once released, the spermatozoa migrate to the ampulla and bind to the zona pellucida [7, 8]. However, the success of direct oviductal insemination via the infundibulum [10] suggests that the ampulla of the oviduct is able to support capacitation and fertilization in the horse.

In vivo studies of the role of the equine oviduct in capacitation and fertilization are unrealistic because they would require invasive surgery or laparoscopy to access the mare's oviduct. To examine how the oviduct supports equine sperm capacitation and fertilization it is, therefore, desirable to establish a representative in vitro oviduct model. Previous studies have largely focused on non-polarized monolayers of de-differentiated OECs [17, 18] and oviduct explant cultures [19]. Unfortunately, neither of these systems was able to support equine IVF. Despite this shortcoming, an oviduct explant model did help to identify physiological conditions triggering three critical hallmarks of stallion sperm capacitation, namely increased intracellular pH [20, 21], protein tyrosine phosphorylation in the sperm tail [20, 21, 22], and hyperactivated motility [22]. However, neither the acrosome reaction nor the fertilization could be induced using oviduct explants. In order to improve in vitro oviduct cell cultures in terms of phenotype and functionality, we and others have recently developed more advanced cell culture models for OECs from the mouse, pig and cow [23, 24, 25]. A monolayer of polarized, differentiated OECs was induced by the introduction of an air–liquid interface [23]. Moreover, in vivo-like functionality of these monolayers could be stimulated by cycle stage-specific concentrations of ovarian steroid hormones [26, 27, 25].

In an attempt to develop an oviduct model to study equine in vitro capacitation and fertilization, this study aimed to establish an advanced in vivo-like equine OEC (EOEC) monolayer using EOECs originating from the ampulla. We further investigated whether the optimal starting material was (1) differentiated, polarized or (2) undifferentiated, non-polarized EOECs. We evaluated two different approaches to colonizing the porous membrane of hanging Transwell inserts, and examined whether the EOEC monolayers established by the two approaches showed in vivo-like cell characteristics. Cell morphology, cell polarization (cell height and primary cilia), monolayer confluency, and the ratio of EOECs with secondary cilia to non-ciliated EOECs were used as criteria. Next, the protocol best supporting rapid EOEC adhesion to the microporous membrane, and confluent monolayer formation after EOEC seeding, was transferred to a microfluidic chip. Finally, the functionality of the re-differentiated EOEC monolayers was assessed by evaluating the effect of cycle stage-specific hormones on nuclear progesterone receptor expression and the capacity for binding stallion spermatozoa.

Materials and methods

Ethical Statement

The study was approved by the Ethical Committees of the Faculty of Veterinary Medicine of Ghent University (EC2013/175 and EC2013/176) and experiments were carried out as approved by the Ethical Committee of the Faculty of Veterinary Medicine of Utrecht University.

Chemicals and reagents

Alexa Fluor 488 conjugated goat-anti-mouse antibodies and phalloidin-Alexa Fluor 568 were obtained from Invitrogen (Landsmeer, The Netherlands). Normal goat serum was purchased from Genway (San Diego, USA). Vectashield was obtained from Vector Laboratories (Peterborough, UK). Triton X-100 and all other chemicals not otherwise specified were obtained from Sigma-Aldrich (Zwijndrecht, The Netherlands).

Animals

Oviducts were collected at a local slaughterhouse within 30 min after the slaughter of healthy Warmblood mares aged between 5 and 22 years, and without any visible reproductive tract pathologies. Oviducts from mares with one or more large follicles and no corpus luteum in the ovaries were considered to be from the follicular phase, whereas oviducts from mares with a corpus luteum in combination with small or large follicles on the ovaries were considered to be from the luteal phase.

Harvesting EOECs

After collection, oviducts were transported within 2 h to the laboratory, on ice, in cold Dulbecco Phosphate Buffered Saline (PBS; 0.9 mM $CaCl_2$, 2.68 mM KCl, 1.47 mM KH_2PO_4, 0.5 mM $MgCl_2$, 137 mM NaCl, 8.1 mM Na_2HPO_4; pH: 7.30, osmolality 300 ± 10 mOsmol/kg; Gibco BRL, Paisley, UK) supplemented with 50 μg/mL gentamycin, 100 U/mL penicillin, and 100 μg/mL of streptomycin.

Upon arrival at the lab, oviducts were dissected free of surrounding tissue, straightened as much as possible, and washed three times in cold calcium- and magnesium-free PBS (Gibco BRL, Paisley, UK) supplemented with 50 μg/mL gentamycin, 100 U/mL penicillin, and 100 μg/mL of streptomycin (antibiotic supplemented calcium- and magnesium-free PBS). In the first experiment, three different EOEC isolation techniques were compared. To standardize the amount of tissue used for cell isolation, each oviduct was first divided into ampullary and isthmic segments of equal length (5 cm each). EOECs were isolated by either (1) oviduct flushing, (2) mechanical isolation, or (3) enzymatic digestion. For oviduct flushing, the lumen of the oviduct segments was flushed three times into a small petri dish (3.5 cm diameter) using 400 μL antibiotic supplemented calcium- and magnesium-free PBS. Any remaining fluid was then gently massaged out of the oviduct segments. An equal volume of HEPES buffered Medium 199 (Gibco BRL, Paisley, UK) containing 50 μg/mL gentamycin, 100 units/mL penicillin, 100 μg/mL streptomycin, and 20% Fetal Bovine Serum (FBS; South American origin, S1141, Greiner Bio-one, Alphen aan den Rijn, The Netherlands) (antibiotic supplemented M199 + 20% FBS) was added to the cell suspension. After flushing, the segments were used for mechanical isolation of cells. For mechanical isolation,

ampullary segments were opened longitudinally inside a sterile flow cabinet, and the mucosa was scraped using the blunt side of a sterile scalpel blade. The blade was rinsed in antibiotic supplemented M199 + 20% FBS. By contrast, cells were massaged out of isthmus segments by squeezing the segment tightly with a dissecting forceps that was advanced from one end to the other. Droplets containing cells were suspended in ~2 mL antibiotic supplemented M199 + 20% FBS. For enzymatic isolation, oviduct segments were first flushed three times with 400 μL antibiotic supplemented calcium- and magnesium-free PBS. Next, the segment was filled with 0.5% Trypsin/0.2% ethylene-diamine-tetra-acetic acid (EDTA; w:v) in PBS and sealed with clamps at each end. The tissue pieces were then incubated for 30 min at 37 °C in antibiotic supplemented calcium- and magnesium-free PBS. After incubation, cells were expelled by massaging the oviduct segments with tightly closed dissecting forceps. Drops containing cells were collected in antibiotic supplemented M199 + 20% FBS. The recovered cells were collected separately for each animal in centrifugation tubes. The tubes were centrifuged (5 min, 300 × g) at room temperature and the supernatant was discarded. The pellet from each tube was suspended in 1 mL M199 supplemented with 10 ng/mL epidermal growth factor, 5 μg/mL insulin, 5 μg/mL apotransferrin, 50 μg/mL gentamycin, 100 U/mL of penicillin, and 100 μg/mL of streptomycin, 1 μg/mL amphotericin B, and 10% FBS (M199 + 10% FBS culture medium). After thorough mixing by pipetting, an aliquot from the cell suspension was removed to assess cell concentration and viability. Cell concentration was determined using a hemocytometer chamber. For viability assessment, the cell suspension was incubated with trypan blue solution (0.4% in 0.85% saline; Gibco BRL, Paisley, UK) at a ratio of 1:1 (v:v) for 4 min at room temperature. At least 100 cells from the isthmus and 200 cells from the ampulla preparations were assessed. Cells stained blue were considered to be dead, whereas white to gray cells were considered alive. For all following experiments, EOECs were isolated by scraping the ampullary oviductal mucosa.

Short-term culture of EOECs

EOECs recovered from ampullary segments were cultured on 12 mm round glass coverslips (Menzel Glaeser, Braunschweig, Germany) in 24 well plates at 37 °C in a humidified atmosphere of 5% CO_2-in-air. The M199 + 10% FBS culture medium was renewed twice a week. After 10 days, EOECs were fixed in 1% paraformaldehyde for 10 min at room temperature. Fixed cells were stored in PBS at 4°C until further processing.

Long-term EOEC culture

For these experiments, EOECs were harvested by scraping the mucosa of oviduct ampullae. The recovered cell suspension was then diluted in antibiotic-supplemented M199 + 20% FBS. Cells were washed twice by centrifugation at 200 × g for 5 min at 25 °C in the latter medium. The cells were then cultured for 24 h in 6-well plates (Greiner Bio-one, Alphen aan den Rijn, The Netherlands) in DMEM/Ham's F12 medium (DMEM/F-12 Glutamax I; Gibco BRL, Paisley, UK) supplemented with 10% (v/v) FBS, 50 μg/mL gentamycin, 100 U/mL penicillin, 100 μg/mL streptomycin, 10 ng/mL epidermal growth factor, 5 μg/mL insulin, 5 μg/mL apotransferrin, and 1 μg/mL amphotericin B (DMEM +10% FBS culture medium). During these 24 h, the EOECs arranged themselves into floating vesicles with outward facing, actively beating cilia, whereas contaminating (mesodermal) fibroblast cells attached to the surface of the polystyrene 6-well plates. The oviduct epithelial vesicles were subsequently collected, centrifuged at 200 × g for 5 min at 25 °C, resuspended in DMEM +10% FBS culture medium and pipetted up and down several times to mechanically separate the cells. The culture medium was adapted from previous publications [17, 28, 29].

Next, EOECs were seeded at a concentration of 0.5×10^6 EOECs per cm^2 onto the microporous membrane of hanging Transwell inserts (CLS3413, polycarbonate membrane, 0.4 μm pore diameter, apical–basolateral compartment volume: 200–800 μL; Costar, Corning, USA) or into microfluidic "chips" (10 001 556, polycarbonate membrane, 0.4 μm pore diameter, apical–basolateral compartment volume: 75–110 μL; microfluidic ChipShop GmbH, Jena, Germany). Two different approaches to establishing a confluent monolayer of polarized, differentiated EOECs were compared. (1) A direct seeding protocol (Figure 1A) in which oviduct epithelial vesicles were directly seeded onto the porous membrane of the hanging Transwell inserts (0.2 x 10^6 EOECs per insert). Four days after seeding, EOECs were attached to the membrane and had formed a confluent monolayer of differentiated and non-differentiated, i.e., freshly divided, EOECs. At this point, an air–liquid interface was introduced, by removing the medium in the apical compartment, in order to maintain the differentiated status of plated, non-divided EOECs and support differentiation of proliferating EOECs. (2) A re-differentiation protocol (Figure 1B) in which de-differentiated EOECs were used to establish a monolayer in hanging Transwell inserts or on the membrane of microfluidic chips. In this re-differentiation protocol, the oviduct epithelial vesicles were first incubated in DMEM + 10% FBS culture medium for 10 days to allow attachment of the EOECs to the bottom of a 6-well plate and the formation of de-differentiated EOEC monolayers. After 10 days, the de-differentiated EOEC monolayers were detached using 0.25% Trypsin/0.1% EDTA (w:v) in PBS. After a 10–15 min incubation at 38 °C in an incubator with a rocking platform, trypsin activity was blocked by adding antibiotic supplemented M199 + 20% FBS medium; the detached EOECs were then washed by centrifugation-resuspension in this medium (200 × g, 5 min). The de-differentiated EOECs were then seeded onto hanging Transwell inserts or microfluidic chips in DMEM + 10% FBS culture medium at a concentration of 0.5×10^6 EOECs per cm^2. Each insert or chip was seeded with EOECs from a single mare. The volume of culture medium in the Transwells was 800 μL in the basal section and 200 μL in the apical part. Culture medium in the basal compartment of the microfluidic chips was refreshed twice during the first 2 days. In both systems, an air–liquid interface was introduced 3 days (chip) or 4 days (insert) after seeding, by removing the culture medium from the apical compartment. This was done to stimulate re-differentiation of the confluent monolayers of EOECs. Any culture medium leaking from the basal to the apical compartment was removed daily until full membrane confluency was achieved (~5–7 days after air–liquid interface introduction, Figure 1B). All cell culture systems were incubated in a humidified atmosphere of 5% CO_2-in-air at 38 °C for up to 60 days after introduction of the air–liquid interface. The culture medium in the basal compartment of

the Transwell insert system was completely refreshed twice a week. In contrast, dynamic medium refreshment of the basal compartment of the microfluidic chips was started 3 days after cell seeding using a Programmable Aladdin Syringe Pump (World Precision Instruments GmbH, Friedberg, Germany) and a constant microfluidic perfusion rate of 5 μL/h.

Immunohistochemistry of reference tissue and EOEC monolayer sections for cell height, ciliation and progesterone receptor expression

Reference tissues for assessing the percentage of ciliated and nuclear progesterone receptor positive EOECs; and cell height were obtained from three mares in each of the follicular and luteal phases. The ampulla of the oviducts was dissected from the remaining tissue and fixed in 4% formaldehyde for 1–3 days. The fixed ampulla was then embedded in paraffin and 3 μm sections were subsequently cut and mounted on Superfrost plus glass slides. Samples were either stained with hematoxylin–eosin (HE), probed without antigen retrieval for the presence of cilia or probed after antigen retrieval for nuclear progesterone receptor expression.

The paraffin-embedded oviduct sections were prepared for HE staining by heating in an oven at 60 °C for 15 min. The sections were then stained with Pas Hematoxylin for 4 min and rinsed with water for 5 min. Next, the sections were incubated successively for 1 min in 70% and 96% ethanol. The sections were then stained with eosin Y for 1 min before dehydration by immersion in 100% ethanol (twice for 1 min) and xylene (twice for 1 min). Slides were sealed with water soluble glue and a coverslip prior to microscopic evaluation of cell height.

Oviduct sections for cilia and nuclear progesterone receptor staining were subsequently deparaffinized using xylene and decreasing ethanol concentrations (first 100%, then 50%). A final wash step was performed using PBS. Next, antigen retrieval was performed for the oviduct sections to be processed for nuclear progesterone receptor staining only. Briefly, antigen retrieval was performed by heating in a citrate buffer (pH 6). The slides were submerged in the buffer, heated to 97 °C and incubated for 20 min. After cooling down to 75 °C, the slides were rinsed thoroughly in PBST for 5 min.

Regardless of whether antigen retrieval was performed, oviduct sections were treated for 5 min with endogenous peroxidase activity blocking solution (S2023; Dako, Heverlee, Belgium). Slides were then washed with PBST and blocked with normal goat serum for 15 min. Next, the anti-acetylated alpha tubulin antibody (sc-23,950, Santa Cruz Biotechnology; 1:200 in normal antibody diluent (33 593; Immunologic, Duiven, The Netherlands)) or the anti-nuclear progesterone receptor antibody (MA5–14505, Thermo Fisher Scientific; 1:200 in normal antibody diluent) was added for 1 h at room temperature. After three washing steps, the horse radish peroxidase-conjugated secondary antibody (concentration indicated by the manufacturer; VWRKDPVO110HRP; Brightvision, Almere, NL) was added to the slides and incubated for 30–60 min at room temperature. The slides were washed again in PBST before 2 drops of the chromogen AEC (K3464; Dako, Heverlee, Belgium) were added. After a 20-min incubation, the slides were rinsed with demineralized water and counterstained with PAS-Hematoxylin (3870, Baker, Landsmeer, The Netherlands). The slides were then rinsed with tap water for 5 min and sealed under a cover slip with water soluble glue (Aquatex; Merck, Amsterdam, The Netherlands). Estrous cycle stage-mimicking hormone exposed EOEC monolayers (see below) were stained, after fixation and paraffin-embedding, for nuclear progesterone receptor expression using a similar protocol.

Brightfield images were taken using an Olympus BX60 microscope at magnifications of 200x, 400x, and 1000x. At three different locations on secondary folds of the reference tissue, 100 cells were assessed for the presence of secondary cilia and nuclear progesterone receptors. The average value of these three locations was considered representative for an individual mare. For EOEC monolayers, 100 EOECs per monolayer were assessed and the percentage of positive cells was determined. Cell height was assessed using Fiji software [30]. Twenty cells from the HE-stained samples that were fully visible from base to the apex were measured. The secondary cilia were not included in the cell height.

Epithelial characterization of EOECs after culture

A marker for cells of epithelial origin (Anti-Cytokeratin 19 antibody, clone b170; ab49384, Abcam, Cambridge, UK) was validated using reference tissue from mares in either the follicular or the luteal phase.

Cryosections of isthmus and ampulla from three different mares ($n = 3$) were cut on a cryostat with a fixed blade (Model CM 3050S, Leica, Eindhoven, The Netherlands) at −20 °C. Fourteen μm thick sections were mounted on Superfrost plus glass slides (VWR, Amsterdam, The Netherlands) and stored at +4 °C until staining. Sections were fixed with acetone for 10 min. After rinsing in PBS with 0.2% (v:v) Tween 20 (PBST), samples were permeabilized and nonspecific binding of the secondary antibody was blocked using 5% normal goat serum (GenWay Biotech, San Diego, CA, USA) in PBST for 30 min. After two washing steps with PBST, the sections were incubated with the primary antibody in PBST (1:50 anti-cytokeratin 19) overnight at 4 °C. Next, the slides were rinsed three times for 5 min with PBST before incubation with the secondary antibody (1:100 in PBST; Goat anti-Mouse IgG (H + L)) conjugated to Alexa Fluor 488, A11029; life technologies) for 1.5 h at room temperature. After another two washes in PBST, sections were stained with Hoechst 33342 (5 μg/mL) and phalloidin conjugated to Alexa Fluor 568 (both at 1:100 dilution (v:v) in PBST). After 1 h incubation at room temperature, sections were rinsed three-times with PBST and covered with a 1:1 mixture of Vectashield (Vector Laboratories, Burlingame, CA, USA) and PBS. A cover slip was applied and sealed with nail polish. The slides were stored in the dark at 4 °C until imaging. During each staining session, one sample was incubated with PBST instead of the primary antibody, and served as negative control.

Glass cover slips with cultured EOECs, and EOEC monolayers cultured by the direct seeding and de-differentiation/re-differentiation protocols were processed as described for tissue sections. The only difference was that cultured EOECs were fixed in 1% paraformaldehyde for 10 min at room temperature.

Sections were imaged using a fluorescence microscope (BX60, Olympus, Zoeterwoude, The Netherlands) equipped with a CCD camera (Leica DFC425C) connected to LAS-AF software (Leica Microsystems GmbH, Wetzlar, Germany) at 100–400x magnification. The light source was an UV lamp (EL-6000, Leica) and filters for blue fluorescence (wavelengths for filters were for excitation: 340–380/20 nm, dichroic mirror: 400 nm, emission: >425 nm), green fluorescence (excitation: 445–535 nm, dichroic mirror: 510 nm,

emission: >515 nm), and red fluorescence (excitation: 515–560 nm, dichroic mirror: 580 nm, emission: >590 nm) were used. During imaging of samples, exposure time, gain, and gamma values for the green fluorescence (cytokeratin labeling) were kept constant between stained samples and the corresponding negative controls, while settings for imaging blue and red fluorescence were adjusted to optimize balance of the color in the overlay images.

Detection methods for confluency in the EOEC monolayer

Trans-epithelial electrical resistance

Trans-epithelial electrical resistance (TEER) measurements were performed as described by Chen et al. [31]. Electrodes (World Precision Instruments GmbH, Friedberg, Germany) were sterilized for 10 min in 70% ethanol connected to a digital Volt-Ohm meter (Millipore, Billerica, USA), and equilibrated according to the manufacturer's recommendations. For assessing the TEER, values in the microfluidic chips two Ag^+/AgCl wire electrodes (World Precision Instruments GmbH, Friedberg, Germany) were connected to the electrodes using alligator clips. To eliminate the influence of temperature and atmospheric conditions, measurements were performed immediately after replacing the DMEM + 10% FBS culture medium with antibiotic supplemented M199 + 20% FBS medium on a heated plate at 38 °C. Using this protocol, no reading drift was apparent. Electrodes were inserted into both the apical and the basal compartment. After 1 min of stabilization, the electrical resistance was recorded. The electrical resistance of a blank insert / chip (without cells) was measured in parallel. To obtain the TEER (in Ω^*cm^2), the blank value was subtracted from the total resistance of the sample, and the final unit area resistance (Ω^*cm^2) was calculated by multiplying the sample resistance by the effective area of porous membrane onto which the EOECs were grown (insert: 0.33 cm^2; microfluidic chip: 0.36 cm^2).

Paracellular tracer flux assay

In addition to TEER measurements, the confluency of the cultured EOEC monolayers was tested using a paracellular tracer flux assay. For permeability measurements, 200 μL of a 12 μg/mL fluorescein disodium salt (0.4 kDa) solution in M199 medium was added to the apical compartment of the hanging Transwell inserts or gently pipetted into the apical channel of the microfluidic chip, and pure M199 medium (without fluorescein) was added or pipetted into the basal compartment. Two hours later, the fluorescence intensity was measured in the medium recovered from the basal compartment of individual inserts or microfluidic chips. Empty devices (no EOECs) served as a control for maximum tracer flux, i.e., 100%. The fluorescence intensity was measured using a BMG Clariostar fluorimeter (Ortenberg, Germany). The permeability values for each monolayer were expressed as relative flux by comparison to the maximum tracer flux in empty devices.

EOECs morphology and ciliation

At designated times after introduction of the air–liquid interface, EOEC monolayers cultured in Transwell inserts and microfluidic chips were assessed for cilia formation, presence of tight junctions and cytokeratin expression. The monolayers were fixed in 4% paraformaldehyde in PBS for 15 min at room temperature and then rinsed twice with PBS for 5 min. Subsequently, the EOECs were permeabilized and non-specific binding was blocked using PBS containing 0.5% Triton X-100 and 5% normal goat serum for 30 min at room temperature. The membranes were washed twice in PBS containing 0.5% Triton X-100 for 5 min. The membranes were then incubated overnight at 4 °C with either a mouse anti-acetylated α-tubulin primary antibody (1:100 dilution, sc-23950; Santa Cruz Biotechnology, Santa Cruz, CA, USA) to stain cilia, a mouse anti-occludin primary antibody (1:100 dilution, ab168957; Abcam, Cambridge, UK) to stain tight junctions, or a mouse anti-cytokeratin 19 antibody (1:50, clone b170; ab49384; Abcam, Cambridge, UK) to verify the epithelial nature of the cultured cells. The next morning the EOECs were washed three times in PBS containing 0.5% Triton X-100 (5 min per wash) and incubated with an Alexa Fluor 488 conjugated goat anti-mouse antibody (1:100 dilution; Invitrogen, Landsmeer, The Netherlands) at room temperature for 2 h. The membranes were washed a further three times with PBS containing 0.5% Triton X-100 for 5 min. Subsequently, cell nuclei and actin filaments were stained respectively using 5 μg/mL Hoechst 33342 and phalloidin conjugated to Alexa Fluor 568 (1:100 dilution) in PBS containing 0.5% Triton X-100. After 1 h incubation, the membranes were washed twice with PBS for 5 min and excised from the hanging insert or chip chamber. Excised membranes were mounted on glass slides (Marienfeld, Lauda-Königshofen, Germany) using Vectashield (Vector Laboratories, Burlingame, USA) as antifade, and sealed with nail polish. Negative controls were prepared by omitting incubation with the primary antibody. Imaging was performed by laser scanning confocal microscopy using a TCS SPE-II system (Leica Microsystems GmbH, Wetzlar, Germany) attached to an inverted semi-automated DMI4000 microscope (Leica) with a 40x objective with a numerical aperture (NA) of 1.25, 63x objective with NA 1.30 or 100x objective with NA 1.40. Z-stacks with 0.21 μm step size and 1.5x digital zoom were obtained. The 3D constructs of the monolayer cells were assembled using ImageJ software (National Institutes of Health, Bethesda, MD, USA) or Leica LAS AF lite software to assess cell morphology and measure cell height. In the direct seeding protocol and in the proof-of-principle experiment for spontaneous re-differentiation of pre-cultured EOECs, two image stacks per timepoint and mare were obtained using the 63 x lens to quantify the percentage of ciliated EOECs. A mean of 106 EOECs (min: 61, max: 166) per stack were evaluated. In the systematic screening experiment, imaging was performed using the epifluorescence microscope described previously, to assess the percentage of ciliated EOECs. The magnification objective was 40x NA 0.75. Five randomly selected fields of view in the center of the membrane were imaged for each monolayer and, at least, 750 EOECs per membrane were classified. The images were imported into Imaris 8.2 software (Bitplane AG, Zurich, Switzerland) to determine the percentage of ciliated EOECs on each membrane. The ratio of nuclei without overlaying cilia to the total number of counted nuclei was assessed.

Effect of cycle stage-mimicking hormone exposure on EOEC monolayers

Evaluation of the presence of nuclear progesterone receptors in EOECs was performed using EOEC monolayers exposed to estrous cycle stage-mimicking hormones. Hormone concentrations resembled concentrations found in oviduct tissue and blood at the respective cycle stage [11, 32, 33]. At the

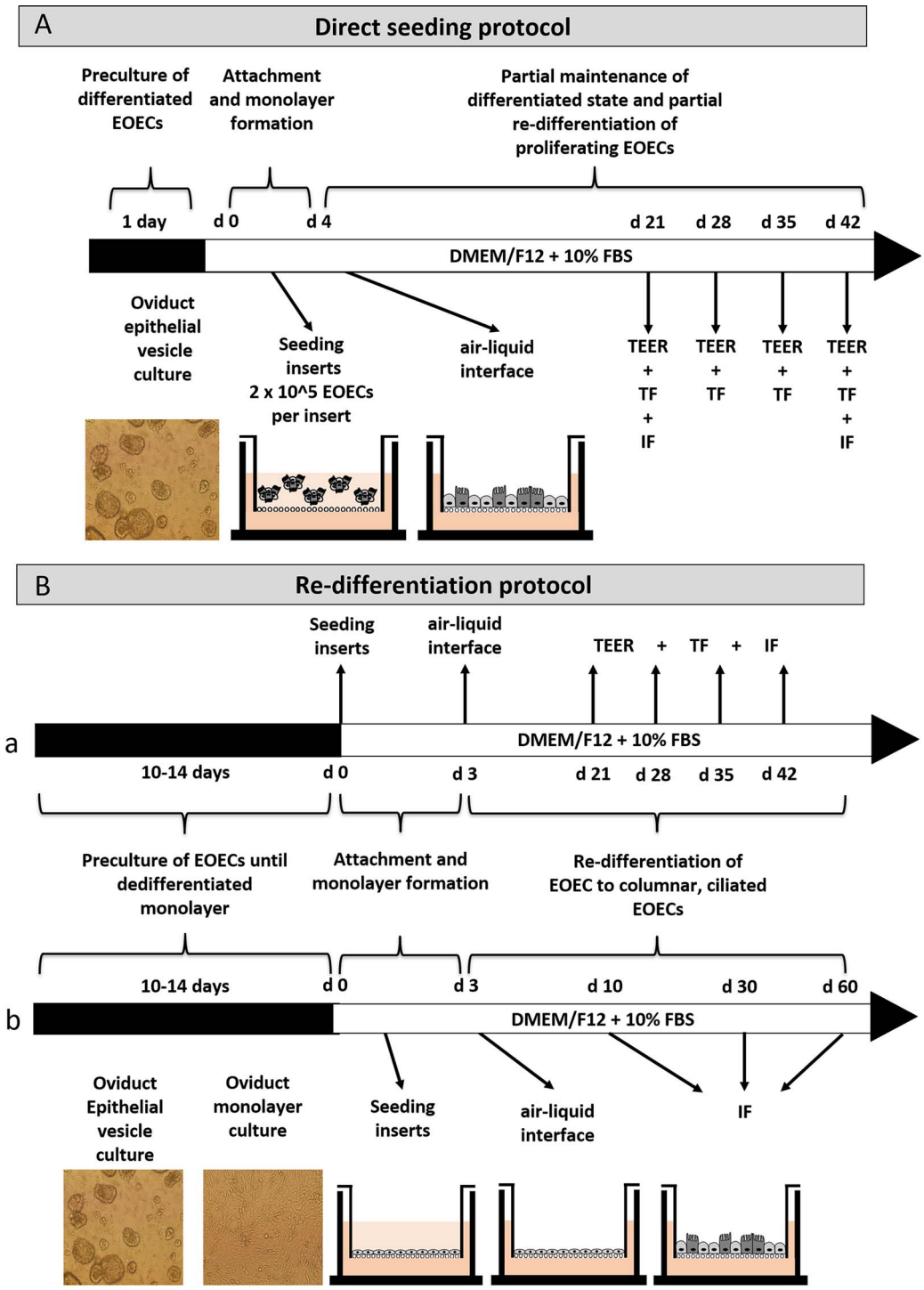

Figure 1. Experimental set-up to establish confluent monolayers of differentiated EOECs on a microporous membrane in Transwell inserts. The re-differentiation of the cultured EOECs was stimulated by the introduction of an air–liquid interface at the apical surface of the monolayers. Two protocols were developed: (A) a direct seeding and (B) a re-differentiation protocol. Re-differentiation experiments were divided in the manuscript into a (a) proof-of-principle experiment and (b) systematic experiments for evaluation of critical factors (FBS: fetal bovine serum; TEER: transepithelial electrical resistance; TF: tracer flux assay; IF: immunofluorescent staining).

time of air–liquid interface introduction EOEC monolayers were cultured in DMEM + 10% FBS culture medium supplemented with E2 (E2; P8783-16, Sigma, Zwijndrecht, The Netherlands) and progesterone (P4; E2758-16, Sigma, Zwijndrecht, The Netherlands) to mimic sequentially the luteal and follicular phases of the mare's estrous cycle. To this end, the medium in the basal compartment was supplemented for 16 days with 10 ng/mL E2 and 1000 ng/mL P4 (oviduct concentration) or 20 pg/mL E2 and 10 ng/mL P4 (blood concentration) to mimic the luteal phase. In order to induce follicular phase conditions, hormone concentrations were changed to 80 ng/mL E2 and 40 ng/mL P4 (oviduct concentration); or 40 pg/mL E2 (blood concentration) for five consecutive days. For sperm-binding experiments, only

oviduct concentrations were assessed. Ethanol served as solvent for the hormone supplementation with a final ethanol concentration of 1% (v:v). Culture medium was refreshed every other day.

Sperm preparation

Semen from two fertile stallions was collected with the help of an artificial vagina (Hanover Model) and a dummy mare. Collected ejaculates were filtered through gauze and diluted with INRA96 (IMV technologies, L'Aigle, France) to a concentration of 30 x 10^6 spermatozoa / mL. Computer-assisted sperm analysis (CASA) was carried out as previously described by Brogan et al. [34]. Only samples with at least 65% motile spermatozoa were used for experiments. Next, spermatozoa were labeled with Hoechst 33342 (final concentration: 5 μg/mL) during incubation for 15 min at 37 °C. The spermatozoa were then layered on top of a discontinuous 35:70% Percoll-saline gradient and centrifuged for 10 min at 300 × g followed by 10 min at 750 × g to remove extracellular Hoechst 33342 dye. The supernatant and Percoll-saline was pipetted off and the sperm pellet was resuspended in a bicarbonate-free variant of Tyrode's medium (111 mM NaCl, 3.1 mM KCl, 0.4 mM $MgSO_4$, 5 mM Glucose, 0.3 mM KH_2PO_4, 20 mM HEPES, 21.7 mM Na-lactate, 1 mM Na-pyruvate, 100 μg/mL gentamycin, 2 mM $CaCl_2$, and 1 mg/mL BSA). The final sperm concentration was adjusted to 10 × 10^6 spermatozoa / mL.

Sperm-binding assay

Binding of spermatozoa to EOEC monolayers exposed to cycle stage-mimicking hormone concentrations was tested at the end of the "luteal" and the end of the "follicular" phase. At both timepoints, semen from both stallions was freshly collected and prepared for the experiments as described above. Hoechst-labeled spermatozoa from the two fertile stallions were mixed equally to reduce any stallion bias on sperm-EOEC binding. Next, 100 μL mixed sperm suspension was added to the apical compartment of the Transwell inserts (10 × 10^6 spermatozoa / mL). Coincubation was carried out for 1 h at 37 °C in 5% CO_2-in-air. Subsequently, the apical compartment was gently rinsed with bicarbonate-free Tyrode's medium to remove non-bound spermatozoa. Samples were fixed with 4% paraformaldehyde for 15 min at room temperature and stained with acetylated α-tubulin (1:150; detected with 1:100 goat-anti-rabbit Alexa Fluor 647) and phalloidin-AlexaFlour 568, in analogy to the immunofluorescent staining procedure described above. Samples were mounted on slides with Vectashield, covered with a cover slip and sealed with nail polish. Five randomly selected spots on each membrane were imaged by fluorescence microscopy (Olympus BX 60, 20x magnification). The number of bound spermatozoa per mm^2 was quantified by the number of bound sperm heads, with the help of the counting tool in Adobe Photoshop (version 2014, Adobe, CA, USA). Results from all five locations per membrane were averaged and considered as the sperm-binding density for a given sample.

Experimental design

In order to investigate EOEC characteristics in reference tissue, paraffin-embedded sections of ampullary origin were initially made from three donors at the follicular and three donors at the luteal stage. EOEC morphology including cell shape and height, ciliated: non-ciliated EOEC ratio and secondary cilia distribution was evaluated.

In a second experiment, three different EOEC collection methods, i.e., conventional oviduct flushing, mechanical isolation, and trypsin digestion were compared for their efficiency in retrieving a population of viable EOECs from the isthmus and ampulla. Cell number and viability of EOECs collected from the isthmus and ampulla were assessed by Trypan Blue staining using a hemocytometer chamber. All values refer to the results from a single 5 cm long oviduct segment. In short, both oviducts from five donors were assessed for the conventional flush technique ($n = 10$); subsequently one of the two oviduct sections was subjected to mechanical scraping ($n = 5$) and the other to enzymatic digestion ($n = 5$).

Next, the epithelial origin of harvested and cultured EOECs recovered from ampullary segments was evaluated by cytokeratin 19 staining after 10-day culture on glass cover slips ($n = 5$ mares; $n = 10$ samples). Likewise, three EOEC monolayers obtained 21 days after air–liquid interface introduction after direct seeding ($n = 5$ mares) or re-differentiation of EOECs ($n = 5$ mares) were evaluated for cytokeratin 19 expression.

Subsequently, differentiated EOEC monolayers were produced in Transwell inserts. Using the direct seeding protocol, 21 days after introduction of an air–liquid interface EOEC morphology, cell height, and primary and secondary ciliation rates were assessed by combined Hoechst 33342, F-actin, and anti-acetylated α-tubulin antibody labeling. Moreover, the confluency of the EOEC monolayers was assessed by TEER and tracer flux measurements 21, 28, 35, and 42 days after air–liquid interface introduction. Timepoint 0 days was not included since EOECs were still in the process of attachment and reaching confluency. All parameters were assessed on five EOEC monolayers per donor. In total, five donors were assessed in this experiment ($n = 25$ inserts per experiment).

Since initial adhesion of the EOECs to the microporous membrane and formation of a confluent monolayer took about 10 days, a de- and re-differentiation protocol, allowing EOEC adhesion within 2 days, was established in Transwell inserts before transfer to microfluidic chips. In a proof-of-principle experiment, similar morphology parameters were assessed 21 days after air–liquid interface introduction. EOEC monolayer confluency was assessed by TEER and tracer flux measurements 0, 21, 28, 35, and 42 days after air–liquid interface introduction. All parameters were assessed on eight EOEC monolayers per donor. In total five donors were assessed in this experiment ($n = 40$ inserts). TEER and tracer flux data could only be collected for four donors at the time due to technical problems with the TEER electrodes. Next, the effect of the cycle stage of cell donor and experiment on the secondary ciliation variability was assessed 1 and 2 months after air–liquid interface introduction. Secondary ciliation rates were assessed for three inserts per donor. In 10 different experiments, a total of 30 different donors were evaluated including 17 mares in the follicular phase and 13 mares in the luteal phase ($n = 90$ inserts).

The functionality of EOEC monolayers cultured by the re-differentiation protocol in Transwell inserts and subsequently exposed to cycle stage-mimicking hormones was evaluated as follows. EOEC monolayers from four different mares were cultured for 16 days in luteal phase hormone conditions followed by 5 days in follicular phase hormone conditions. We examined whether mimicking both the luteal and follicular phases of the cycle, and comparing oviduct and blood hormone concentrations, would have an effect on nuclear

progesterone receptor expression. For each of the four donors, one EOEC monolayer was assessed. For the sperm-binding assay, EOECs were collected from three different donors. Two monolayers per donor and per simulated cycle stage were assessed. In total, 12 inserts were assessed in this experiment. The number of bound spermatozoa was counted for five randomly selected spots per Transwell insert.

Finally, the de- and re-differentiation protocol was transferred to microfluidic chips since EOEC adhesion allowed early onset of microfluidic perfusion, within 2–3 days after seeding. The effect of EOEC donor cycle stage on the variability of secondary ciliation was assessed 1 and 2 months after air–liquid interface introduction. Secondary ciliation rates were assessed for two inserts per donor. Within five different experiments, a total of 10 different donors were evaluated, including six mares that were in the follicular phase and four mares in the luteal phase ($n = 20$ inserts).

Statistical analysis

All experiments were performed with EOECs from different Warmblood mares in duplicate or triplicate. Before analysis, normality of distribution for the variables was checked using the Shapiro–Wilk and Kolmogorov–Smirnov tests ($P < 0.05$). Differences between isolation protocols in EOEC yield and viability were evaluated with the Mann–Whitney *U*-test. The relationship between TEER and paracellular tracer flux was modeled by non-linear regression. Correlations between cell density and the percentage of ciliated EOECs were calculated using Spearman correlation coefficient. An effect of culture time on TEER was estimated using a one-way-ANOVA for repeated measures. Student *t*-test for paired observations was used as a post-hoc test. The effect of both protocols on membrane confluency parameters; presence of primary and secondary cilia in EOECs cultured in the two different systems; expression of nuclear progesterone receptors and sperm–binding density to EOEC monolayers exposed to cycle stage-specific hormones were assessed by analysis of variance (ANOVA). Overall differences were identified using repeated measures ANOVA with Greenhouse–Geisser and Bonferroni correction, as implemented in the general linear model. Scheffé post-hoc tests were performed for pairwise comparisons. Differences were considered significant if $P < 0.05$. All analyses were performed using SPSS version 20 for Windows (SPSS Inc., Chicago, IL).

Results

EOEC morphology in reference tissues

Paraffin-embedded oviduct sections of ampullary origin demonstrated that the luminal lining is composed of columnar EOECs that are either non-ciliated or have a bundle of secondary cilia on their apical side (Figure 2A). Immunohistochemistry using anti-acetylated alpha tubulin antibodies demonstrated the distribution of secondary cilia at the level of the ampulla (Figure 2B). The percentage of secondary ciliated EOECs was $60 \pm 14\%$ in the follicular and $55 \pm 10\%$ in the luteal phase. Moreover, nuclear progesterone receptors were present in ampullary EOECs (Figure 2C). In total, $60 \pm 10\%$ and $63 \pm 14\%$ of the EOECs from luteal and follicular phase oviducts, respectively, demonstrated progesterone receptor expression in their nucleus. Average cell height was 12.8 ± 1.5 μm in the follicular and 16.0 ± 4.7 μm in the luteal phase. Occasionally, cell bodies protruded beyond the epithelial lining. In most cases, these protrusions contained nuclear material (Figure 2A).

Viable EOECs can be collected from the ampulla by mechanical scraping or trypsin digestion

EOECs were collected from the ampulla and the isthmus by three different methods. Conventional oviduct flushing resulted in extremely low EOEC yields from both the ampulla (5 ± 6 x 10^3 total live cells) and the isthmus (5 ± 5 x 10^3 total live cells) (Table 1). The mechanical isolation and trypsin digestion methods were equally successful for retrieving EOECs from the ampulla (25.5 ± 22.0 x 10^6 vs 31.7 ± 16.6 x 10^6 total live cells) (Table 1). By contrast, trypsin digestion was five times more effective than mechanical isolation for collecting viable cells from the isthmus (4.15 ± 4.93 x 10^6 vs 0.86 ± 0.62 x 10^6 total live cells; Table 1).

Harvested and cultured cells are of epithelial origin

Monolayers obtained by 10-day culture on glass cover slips of EOECs recovered from ampullary segments (Figure 3A), and EOEC monolayers obtained 21 days after air–liquid interface introduction after direct seeding (Figure 3B) or re-differentiation of EOECs (Figure 3C) all stained positive for cytokeratin 19, an epithelial cell marker (Figure 3). Oviduct cryosections taken at the level of the ampulla, and containing EOECs on the luminal side, were used as a positive control and showed similar specific EOEC cytokeratin 19 staining (Figure 3D). Negative controls (secondary antibody only) showed no fluorescence (Figure 3A-D).

Establishment of differentiated EOEC monolayers in Transwells can be achieved by direct seeding or by de- and re-differentiation

Using the direct seeding protocol, a confluent EOEC monolayer with ciliated and non-ciliated cells was obtained ~21 days after air–liquid interface introduction (Figure 4A). All EOECs contained an intact round or oval-shaped nucleus at the basal end of the cell (labeled with Hoechst 33342) and a dense cytoskeleton as observed using phalloidin (F-actin) labeling (Figure 4A and B). An average cell height of 13.2–18.5 μm (21 days; Figure 4H) and 19.6–30.2 μm (42 days) indicated their columnar shape. In addition, between 44 and 70% and 5 and 22% of the EOECs in the monolayers displayed primary and secondary cilia on their apical surface at Day 21, respectively (Figure 4F and G). During prolonged culture, the percentage of primary and secondary ciliated EOECs increased from 61 to 80% and 31–46% in 3 out of 5 mares, respectively (42 days). The ciliated EOECs were distributed diffusely over the monolayer (Figure 4A and B). However, the percentage of ciliated EOECs correlated significantly with EOEC density on the microporous membrane (EOECs per mm^2; $r = 0.78$, $P < 0.05$). In order to confirm monolayer confluency, TEER was assessed in EOEC monolayers 21, 28, 35, and 42 days after air–liquid interface introduction. In general, TEER increased slightly between Days 28 and 35 (Figure 4C). However, TEER measurements showed a wide variation between individual mares, and between different monolayers derived from individual animals (Figure 4D). Nevertheless, monolayer integrity or confluency was confirmed by low paracellular tracer flux (<5%). Based on pooled results from Days 21

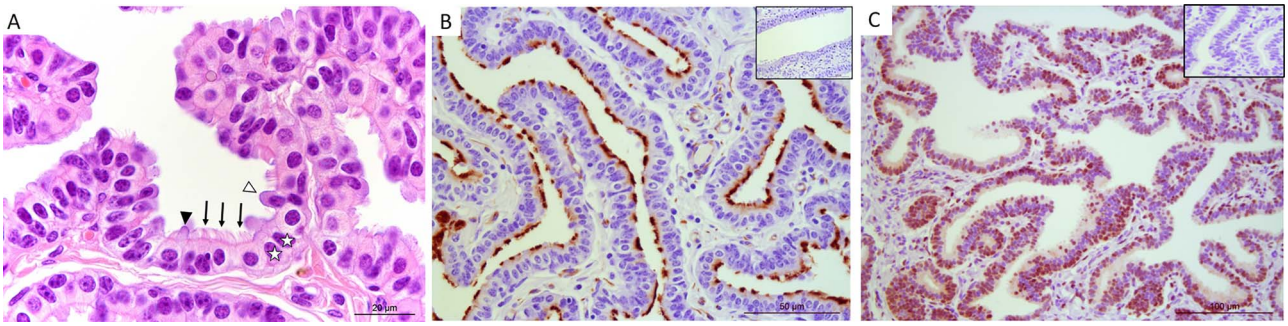

Figure 2. (A) Morphology of EOECs at the level of the ampulla, stained with HE (1000x). Black arrows indicate secondary ciliated EOECs and white stars demonstrate non-ciliated EOECs. The black arrow head shows an apical protrusion, while the white arrow head shows an apical protrusion with a nucleus. Sections of the equine oviduct ampulla after immunohistochemical staining for (B) acetylated alpha tubulin (400x) and (C) nuclear progesterone receptors (200x). Secondary cilia and nuclei positively stained for progesterone receptors show a distinct brown staining pattern. Inlays are negative control images.

Table 1. Comparison of methods for isolating OECs from equine oviducts OECs were harvested by (A) flushing the oviductal lumen with PBS (flush), (B) scraping the mucosa of the longitudinally incised ampulla, or squeezing the isthmus with forceps (mechanical), or (C) by filling the lumen with Trypsin/EDTA for 30 min at 38 °C and subsequent mechanical isolation (Trypsin). Cell number and viability (mean ± s.d.) were assessed after Trypan Blue staining using a hemocytometer chamber. Different small letters (a,b,c) per column indicate significant differences between isolation methods for EOECs from either ampulla or isthmus ($P < 0.05$).

	Isolation method	Total cell number (x10^6)	Live cells (%)	Total live cells (x10^6)
Ampulla	Flush	0.09 ± 0.06^a	7.4 ± 11.9^a	0.005 ± 0.006^a
	Mechanical	43.1 ± 33.8^b	72.3 ± 30.9^b	25.5 ± 22.0^b
	Trypsin	43.0 ± 21.6^b	75.1 ± 14.6^b	31.7 ± 16.6^b
Isthmus	Flush	0.08 ± 0.04^a	5.3 ± 3.6^a	0.005 ± 0.005^a
	Mechanical	1.10 ± 0.70^b	73.2 ± 26.3^b	0.86 ± 0.62^b
	Trypsin	7.58 ± 6.76^c	50.8 ± 33.6^b	4.15 ± 4.93^c

and 42 ($n = 47$ samples; 2–3 samples per mare) presented in Figure 4E, cultured EOEC monolayers were considered fully intact and confluent when TEER values were >219 Ω*cm^2.

In a proof-of-principle experiment, we demonstrated that spontaneous re-differentiation of pre-cultured de-differentiated EOEC monolayers was possible (Figure 5). Samples from four mares were seeded in Transwell inserts and monitored for up to 6 weeks (42 days) after air–liquid interface induction. Samples were regularly assessed for TEER which, in general, did not fluctuate markedly over time (Figure 5A). On the other hand, samples showed a wide variation between individual mares, and differences in TEER were also observed between samples from individual animals (Figure 5B). Based on the assumption that a paracellular tracer flux lower than 5% confirms an intact/confluent monolayer, TEER values of more than 462 Ω*cm^2 were concluded to be indicative of intact monolayers (Figure 5C). This assumption was strengthened by the presence of a dense occludin band, indicating the presence of tight junctions, towards the apical aspect of the cells (Figure 5C). The proportion of EOECs with secondary cilia after 42 days at an air-liquid interface varied markedly between samples (0–32%; Figure 5D). An example of a monolayer with successful spontaneous phenotypic re-differentiation from de-differentiated EOECs to a columnar ciliated EOECs is depicted in Figure 5E. As an example, a 3D-reconstruction of such a monolayer is provided in Supplemental Video clip 1.

We next investigated whether cycle stage of the cell donor could explain the variability observed. In total, samples from 30 mares were precultured (Figure 6Aa-c) and subsequently seeded onto inserts and cultured for up to 2 months after air–liquid interface introduction (Figure 6Ad-f). One month after air–liquid interface introduction, re-differentiated EOECs had average heights of 18–25 μm and a columnar shape (Figure 6C). The monolayers consisted of columnar/polarized EOECs expressing primary cilia (99.1 ± 0.7%; Figure 6Ae, Af, and B); however, very few EOECs developed secondary cilia after introducing an air–liquid interface (0.9 ± 0.6% of the EOECs in a cultured monolayer; Figure 6Ae and B; Table 2). Very occasionally (5.6% of the cultured monolayers; Table 2), monolayers of re-differentiated columnar/polarized EOECs exhibited significantly higher incidences of secondary ciliation (14.1 ± 4.1%; Figure 6Af and B; Table 2). Even then, EOECs with secondary cilia were distributed diffusely (Figure 6Af) and correlated significantly with EOEC density on the microporous membrane (EOECs per mm^2; $r = 0.80$, $P < 0.05$). Interestingly, there was no significant effect of experiment, cell donor (mare) or cycle stage on secondary ciliation rates (Table 2). Regardless of whether monolayers contained a low or high rate of EOECs with secondary cilia, all cells had a round to oval shaped nucleus and a dense cytoskeleton (Figure 6Ae and Af). Monolayer confluency was confirmed by high TEER values (742 ± 125 Ω/cm^2) and low tracer flux (<5%) measurements 7 days after air–liquid interface introduction. Importantly, no significant differences in confluency parameters were observed between one and two months of culture at an air–liquid interface.

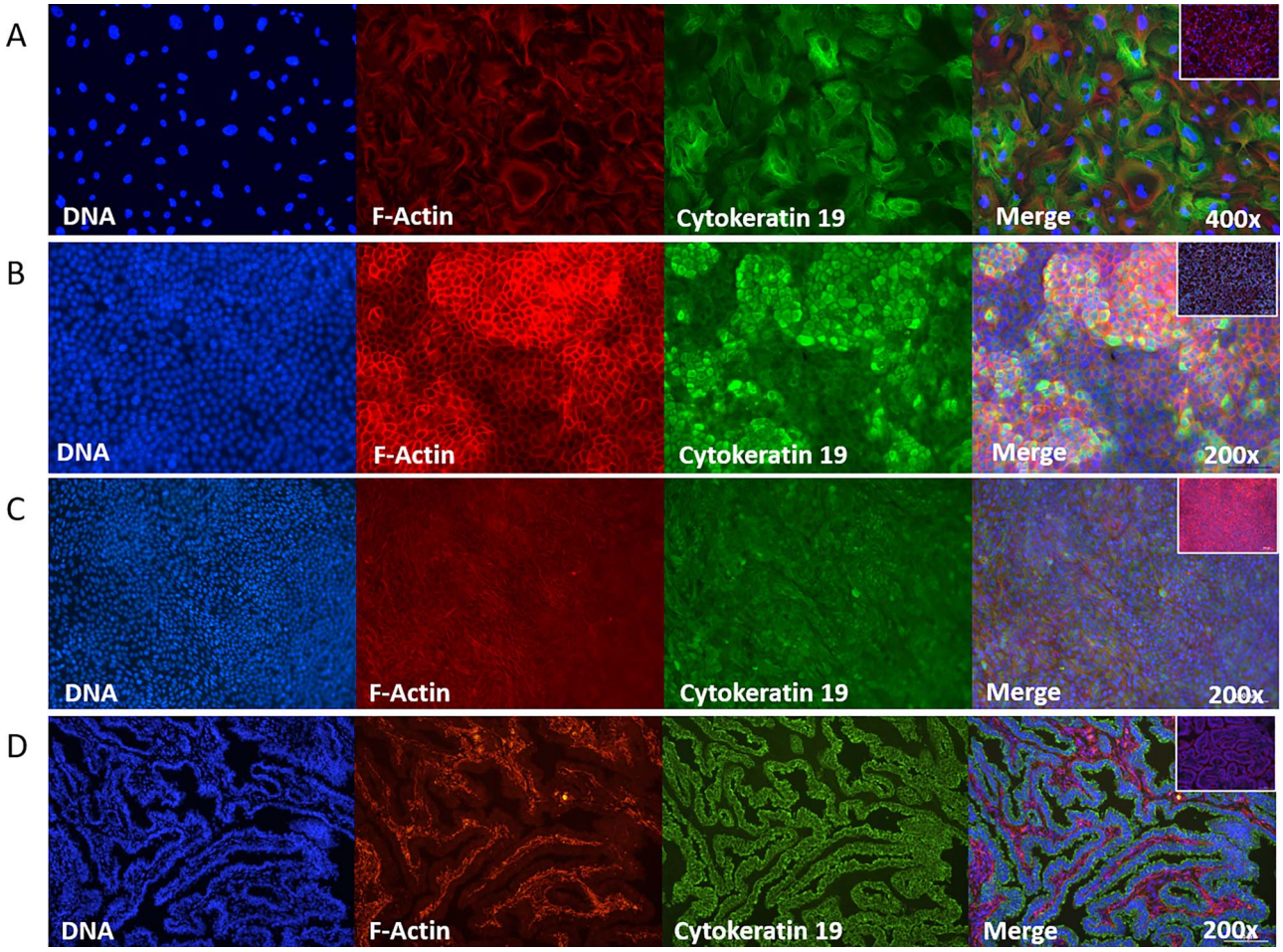

Figure 3. Confirmation that isolated and cultured EOECs of ampullary origin express epithelial cell markers. Indirect immunofluorescent staining for cytokeratin 19 (1:50) was performed. Monolayers obtained after (A) 10 day culture in 6-well plates on glass cover slips, 21 days after air–liquid interface introduction after seeding of (B) differentiated and (C) de-differentiated EOECs, all stained positive for cytokeratin 19 (green, original magnification: 200–400x). (D) As a positive control, histological sections of the oviductal lumen at the level of the ampulla demonstrated that it is lined with cytokeratin 19 positive EOECs. Inlay images (A-D) are negative control samples. EOECs were also stained for DNA (blue) and the cytoskeleton (red: F-actin).

Functionality of re-differentiated EOEC monolayers cultured in Transwell inserts and exposed to cycle stage-specific hormones

Re-differentiated EOEC monolayers cultured for 16 days under luteal hormone conditions showed a low percentage of EOECs expressing nuclear progesterone receptors (oviduct concentration: $13.3 \pm 5.4\%$; blood concentration: $10.5 \pm 6.5\%$) (Figure 7B). By contrast, subsequent culture of EOEC monolayers for 5 days under follicular phase hormone conditions increased the percentage ($P < 0.05$) of EOECs staining positively for nuclear progesterone receptors to ~30% (oviduct concentration: $27.3 \pm 16.5\%$; blood concentration: $30.0 \pm 14.3\%$) (Figure 7A and B). No differences were observed in the percentage of nuclear progesterone receptor positive EOECs between monolayers cultured under oviduct versus blood hormone concentrations in either follicular or luteal conditions (Figure 7B). Overall, these results suggest a significant functional downregulation of nuclear progesterone receptors in EOECs under luteal phase hormone conditions (i.e., high progesterone).

EOECs were able to bind spermatozoa (Figure 8A). Moreover, sperm-binding density was significantly lower for EOEC monolayers exposed for 16 days to luteal conditions (388 ± 87 sperm per mm^2) compared to monolayers exposed for an additional 5 days to follicular phase conditions (1639 ± 389 sperm per mm^2) (Figure 8A, Ba, and Bb, $P < 0.05$). Interestingly, sperm–oviduct binding experiments also showed that spermatozoa bind to cilia located on the surface of the EOEC monolayers (Figure 8Ba and Bb).

Establishing a monolayer of differentiated EOECs in a microfluidic chip can only be achieved via re-differentiation

Oviduct epithelial vesicles were not able to attach to the porous membrane of the chips and form a monolayer in less than 10 days. This may be due to the small volume of medium in the basal compartment of the microfluidic chips, which had to be refreshed at least twice per day. Moreover, to guarantee the supply of fresh culture medium it was important to initiate microfluidic chip perfusion within 2–3 days after seeding. This requirement for the early onset of microfluidic perfusion, i.e., before firm oviduct cell attachment to the membrane, presumably explains failure to allow establishment of a confluent monolayer, or even early cell attachment (Figure 9Aa). Consequently, the direct seeding protocol was not applicable for establishing a differentiated EOEC monolayer culture in microfluidic chips.

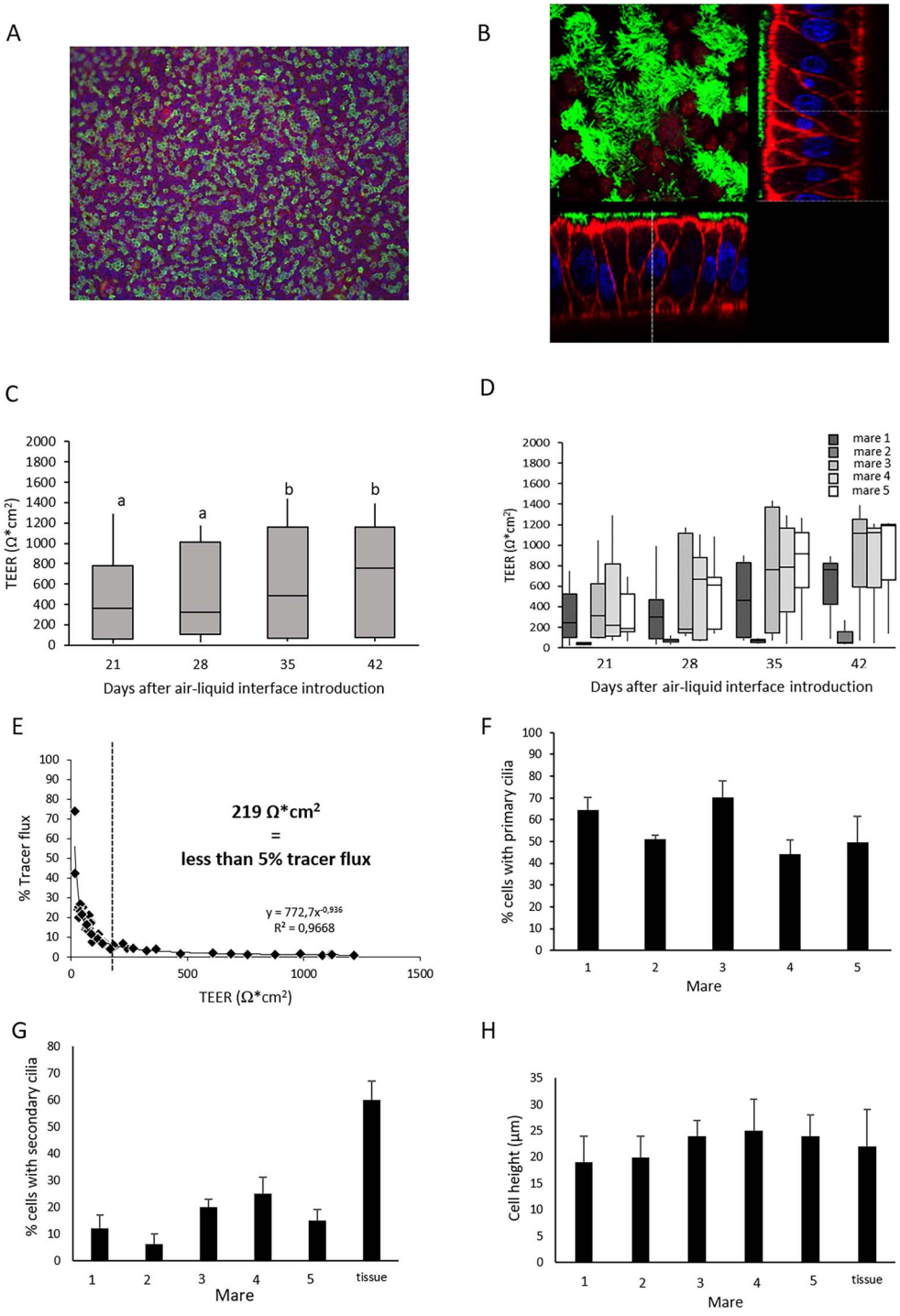

Figure 4. Monolayers of EOECs 21 days after air–liquid interface introduction to cells seeded directly into Transwell inserts (direct seeding protocol). (A) Representative overview image of a cultured monolayer of EOECs 21 days after air–liquid interface introduction (200x). EOECs were stained for markers of cilia (green: acetylated alpha tubulin), DNA (blue) and the cytoskeleton (red: F-actin). (B) A *z*-projection of a typical monolayer demonstrated clear presence of secondary cilia (green: acetylated α-tubulin) and a columnar epithelial cell phenotype (red: F-actin; blue: DNA; original magnification, 945x). (C) TEER measurements (mean ± s.d.) were performed on monolayers of differentiated EOECs cultured in Transwell inserts 21, 28, 35, and 42 days after air–liquid interface introduction (five mares: five inserts per mare). Small letters (a, b) indicate significant differences between days ($P < 0.05$; Student *t*-test for paired samples). (D) The individual effect of these five different mares on TEER values was also verified. (E) The relationship between TEER and flux of Na-fluorescein (0.4 kDa size) across the cultured monolayers was assessed ($n = 47$ assessments pooled from Days 21 to 42). Percentage (mean ± s.d.) of EOECs with (F) primary and (G) secondary cilia in the monolayers. (H) The cell height (mean ± s.d.) of cultured EOECs from individual mares. Reference values (tissue) for the percentage of ciliated EOECs and cell height in the ampulla segment were obtained from three mares ($n = 3$) in each of the follicular and luteal phases. For a schematic overview of the experimental timeline, see Figure 1A.

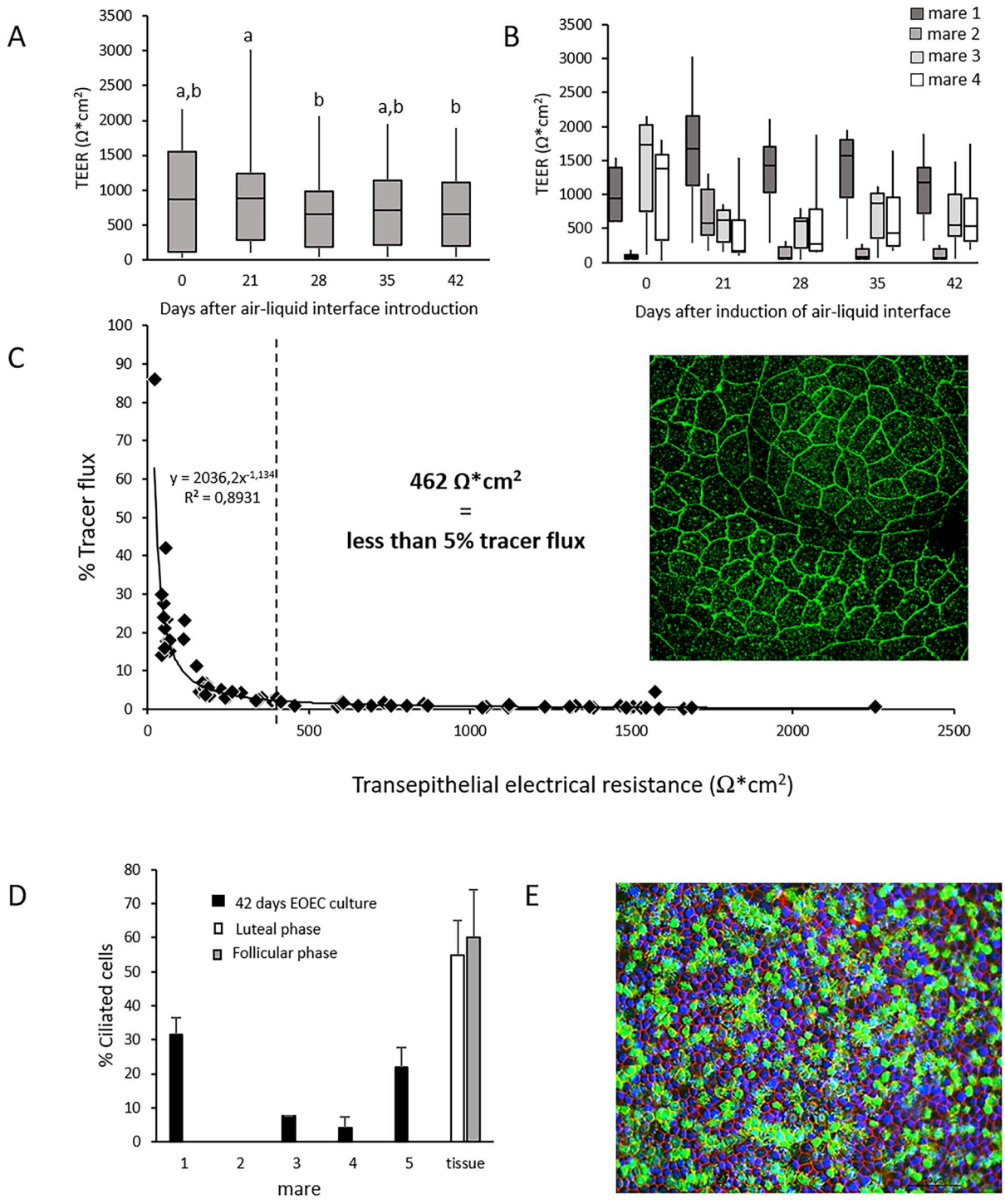

Figure 5. Proof-of-principle experiment for spontaneous re-differentiation of EOECs and quality assessment of EOEC monolayers. Monolayer confluency was assessed by TEER and paracellular tracer flux measurements. (A) TEER measurements (mean ± s.d.) of monolayers of re-differentiated EOECs cultured in Transwell inserts were performed 0, 21, 28, 35, and 42 days after air–liquid interface introduction for four mares (eight inserts per mare). Small letters (a, b) indicate significant differences between days ($P < 0.05$; Student t-test for paired samples). (B) The individual effect of these four different mares on TEER values was also verified. (C) A clear relationship between the overall TEER and paracellular tracer flux results was evident. TEER values of 462 Ω/cm^2 corresponded with less than 5% tracer flux ($n = 72$ assessments pooled from Days 0 to 42). Presence of tight junction complexes was demonstrated by a dense band of occludin (green, original magnification: 945x). (D) Expression of secondary cilia (mean ± s.d.) of EOECs 6 weeks (42 days) after introduction of an air–liquid interface differed between samples. (E) Overview of a monolayer with 26% EOECs with secondary cilia (green: cilia, red: F-actin, blue: DNA; original magnification: 200x). For a schematic of the experimental timeline, see Figure 1Ba.

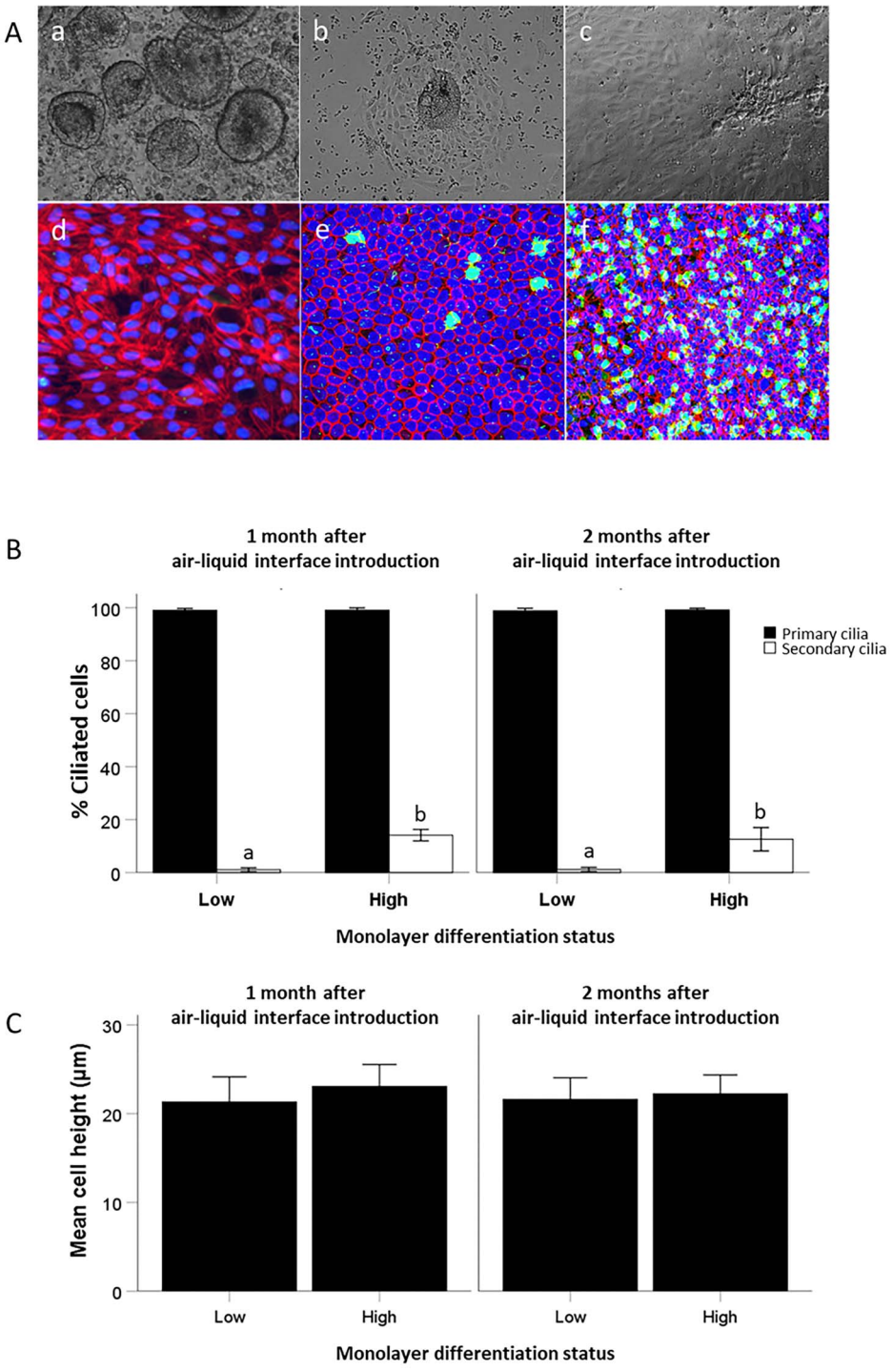

Figure 6. (A) Illustration of the re-differentiation protocol: Representative phase contrast images of (a) oviduct epithelial vesicles at day 1 of culture (200x), (b) attached vesicles with outgrowth of EOECs at Day 3 of culture (150x) and (c) confluent oviduct monolayer of de-differentiated EOECs on Day 10 of culture in 6-well plates (200x). Fluoresence microscopic images represent (d) a re-established monolayer of flat de-differentiated EOECs in Transwell inserts before air–liquid interface introduction, which did not show primary and secondary cilia, (e) a monolayer of columnar-polarized EOECs showing primary cilia and a few secondary cilia after introducing an air–liquid interface and (f) an exceptional (<2%) monolayer of columnar-polarized EOECs showing primary and secondary cilia (13.8%) [green (anti-acetylated α-tubulin antibodies-AlexaFluor 488 secondary antibody): primary (single green dots at each EOEC) and secondary cilia (many green dots on some EOECs), red (phalloidin conjugated to Alexa Fluor 568): cytoskeleton, blue (Hoechst 33342): nuclei] (original magnification, 400x). (B) The percentage of EOECs (mean ± s.d.) with primary and secondary cilia from monolayers with a low or high rate of spontaneously differentiated EOECs 1 and 2 months after air–liquid interface introduction. Significant differences in the percentage of EOECs with secondary cilia are indicated by different small letters ($P < 0.05$). (C) The cell height (mean ± s.d.) from low and high spontaneously differentiated monolayer EOECs was measured from five different mares for both monolayer types. For a schematic overview of the experimental timeline, see Figure 1Bb.

Table 2. Relationship between experiment, cell donor (mare), cycle stage, and secondary ciliation rates 1 month after air–liquid interface introduction in EOEC monolayers cultured in Transwell inserts.

Experiment	Mare	Cycle stage	Insert 1	Insert 2	Insert 3	Mean per mare	Mean per experiment	Mean per cycle stage
1	1	Follicular	1.2	1	0.5	0.9	0.4	
	2	Luteal	0.1	0	0.2	0.1		
	3	Follicular	0.1	0.2	0	0.1		
2	4	Luteal	0	0	0	0.0	0.7	
	5	Follicular	1.3	1.2	1	1.2		
	6	Follicular	0.9	0.6	1.2	0.9		
3	7	Luteal	0.5	0.5	0.5	0.5	0.4	Luteal 1.4 ± 2.9
	8	Luteal	0.2	0.5	0	0.2		
	9	Follicular	0.4	0.3	0.8	0.5		
4	10	Luteal	0.2	0.4	*10.5*	3.7	1.8	
	11	Follicular	0.5	0.5	0.6	0.5		
	12	Luteal	1	1.2	1.3	1.2		
5	13	Follicular	1.2	*13.5*	0.5	5.1	4.5	
	14	Follicular	1.1	0.5	1.3	1.0		
	15	Follicular	*20.2*	1.5	1	7.6		
6	16	Luteal	1.5	1.5	1.9	1.6	1.5	
	17	Luteal	1.2	0.8	0.9	1.0		
	18	Follicular	1.9	2	1.8	1.9		
7	19	Follicular	0.8	1.3	1.2	1.1	1.3	
	20	Follicular	0.9	1.2	1.5	1.2		
	21	Luteal	1.2	1.8	1.5	1.5		
8	22	Follicular	0	0.1	0	0.0	1.0	Follicular 1.8 ± 3.5
	23	Follicular	0.9	1	1.8	1.2		
	24	Follicular	1.8	1.8	2	1.9		
9	25	Luteal	0.5	1.2	1.1	0.9	3.6	
	26	Luteal	*15.8*	0.9	0.8	5.8		
	27	Follicular	0.2	*10.5*	1.2	4.0		
10	28	Luteal	0.5	1.1	0.9	0.8	1.2	
	29	Follicular	1.5	1.2	1.8	1.5		
	30	Luteal	1.8	1.2	0.6	1.2		

On average, 5.6% (5 out of 90 inserts) of the cultured monolayers were classified as "high spontaneous differentiation," whereas 94.4% were classified as "low spontaneous differentiation." Moreover, mean (±s.d.) secondary ciliation rates in the low spontaneous differentiation monolayers was $0.9 \pm 0.6\%$, whereas in the high spontaneous differentiation monolayers it was $14.1 \pm 4.1\%$. No differences were observed between monolayers cultured from EOECs harvested from follicular ($n = 51$) and luteal phase ($n = 39$) oviducts. No significant effect of experiment, mare, and cycle stage on secondary cilia formation was observed ($P > 0.05$). Italic numbers refer to EOEC monolayers considered as high spontaneous differentiated monolayers. Non-italic numbers refer to EOEC monolayers considered as low spontaneous differentiated monolayers.

In contrast, trypsinized, de-differentiated EOECs were able to attach to chip membranes within 2–3 days after seeding. Microfluidic perfusion could therefore be initiated at 3 days after cell seeding. The resulting cultured EOEC monolayers had very similar characteristics to those cultured in hanging inserts (Figure 9Ab, Ac, and B). One month after air–liquid interface introduction, the timespan required for cell re-differentiation, the EOECs had average heights of 20–25 μm and were columnar in shape (Figure 9C). At this time, $99.3 \pm 0.7\%$ of the monolayer EOECs displayed a primary cilium at their apical aspect (Figure 9B). However, very few EOECs demonstrated secondary cilia, despite 30-day exposure to the air–liquid interface ($0.8 \pm 0.6\%$; Figure 9Ab and B). Only two monolayers (10% of all cultured monolayers; Table 3) were observed with a significantly higher proportion of EOECs with secondary cilia (16.8 and 27.4%) (Figure 9Ac and B, Table 3). No significant effect of experiment, cell donor (mare) or cycle stage at oviduct recovery on secondary ciliation rates were observed (Table 3). All EOECs contained a round to oval-shaped nucleus at the basal aspect of the cell and a dense cytoskeleton (Figure 9b and c). TEER measurements were very low ($24 \pm 4\ \Omega/cm^2$ after 1 month; $23 \pm 4\ \Omega/cm^2$ after 2 months of air–liquid interface) when monolayers were cultured in the microfluidic chips. However, low paracellular tracer flux measurements (<5%) obtained 1 and 2 months after air–liquid interface introduction indicated that the EOEC monolayers in microfluidic chips were confluent. As before, no differences in assessed parameters were observed between 1 and 2 months after air–liquid interface introduction.

Discussion

In mammalian species such as the horse, the oviductal ampulla is the site where the oocyte and spermatozoon meet to achieve fertilization. To date, equine ex vivo oviduct models have failed to support sperm capacitation and fertilization. In this study, an improved functional oviduct model was developed that should more closely recapitulate the oviduct luminal environment. Here we produced confluent monolayers of differentiated EOECs in two different ways, i.e., (1) by direct seeding of differentiated EOECs onto the membrane of a hanging insert and (2) by first allowing collected EOECs to form de-differentiated monolayers and subsequently stimulating re-differentiation by introducing an air–liquid interface. The morphology of the EOECs cultured by both approaches was very similar to the in vivo situation, with the distinct

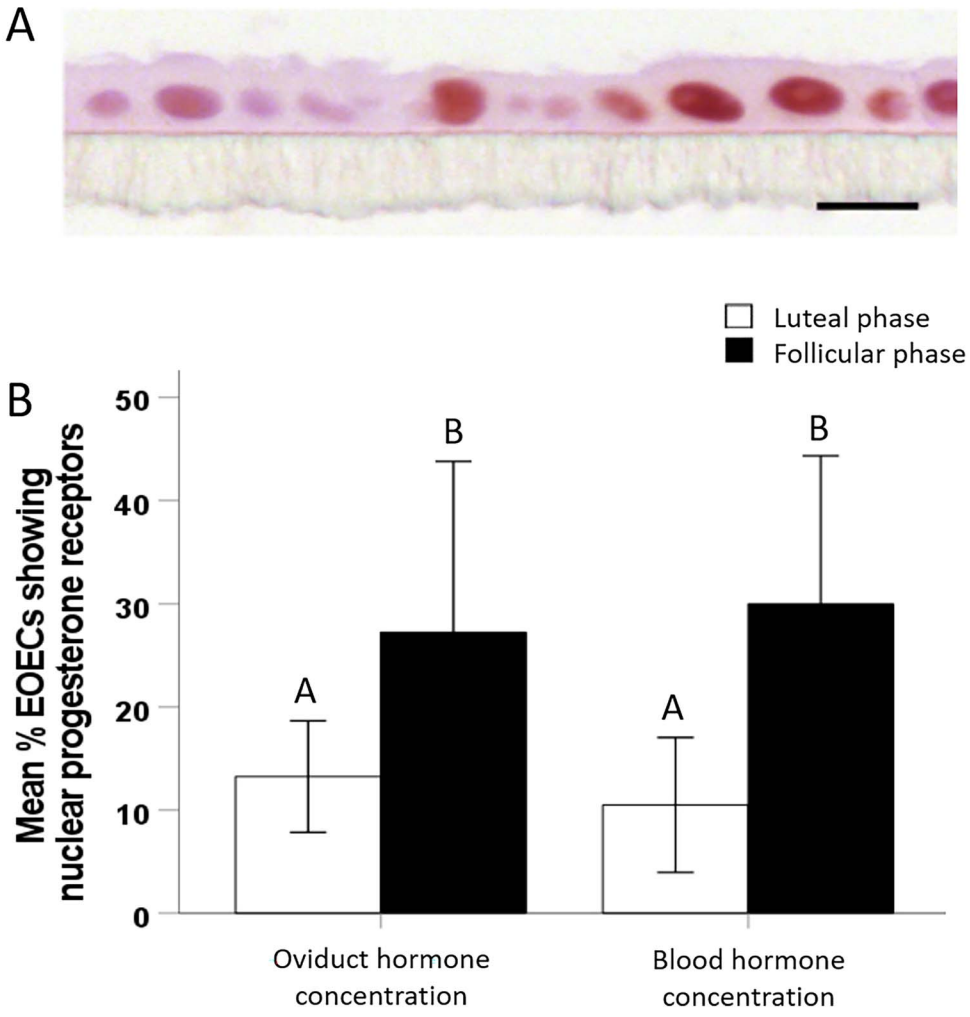

Figure 7. (A) Illustration of an EOEC cultured monolayer exposed to follicular phase mimicking hormone concentrations stained for nuclear progesterone receptors (1000x). (B) Percentage of monolayer EOECs (mean ± s.d.) demonstrating a nucleus positively stained for progesterone receptors after culture under air–liquid interface conditions and exposure for 16 days to luteal phase oviduct (10 ng/mL E2 and 1000 ng/mL P4) and blood (20 pg/mL E2 and 10 ng/mL P4) hormone concentrations; and five consecutive days to follicular phase oviduct (80 ng/mL E2 and 40 ng/mL P4) and blood (40 pg/mL E2) hormone concentrations. Significant differences in the percentage of EOECs showing nuclear progesterone receptors are indicated by different capital letters ($n = 4$, $P < 0.05$).

Table 3. Relationship between experiment, cell donor (mare), cycle stage, and secondary ciliation rates 1 month after air–liquid interface introduction in EOEC monolayers cultured in microfluidic chips.

Experiment	Mare	Cycle stage	Chip 1	Chip 2	Mean per mare	Mean per experiment	Mean per cycle stage
1	1	Follicular	0.6	1.2	0.9	0.9	
	2	Luteal	0.1	1.6	0.9		
2	3	Luteal	1.3	1	1.2	0.6	Luteal
	4	Follicular	0	0	0.0	3.1 ± 5.6	
3	*5*	Luteal	*16.8*	2.1	9.5	6.1	
	6	Follicular	0.2	0.5	0.4		
4	7	Follicular	0.9	0.4	0.7	3.5	Follicular
	8	Follicular	1.2	0.5	0.9		2.8 ± 7.7
5	9	Follicular	1.2	*27.4*	14.3	4.1	
	10	Luteal	1.1	0.5	0.8		

On average, 10% (2 out of 20 inserts) of the cultured monolayers were classified as "high spontaneous differentiation," whereas 90% was classified as "low spontaneous differentiation." Moreover, mean (±s.d.) secondary ciliation rates in the low spontaneous differentiation monolayers was 0.8 ± 0.6%, whereas in the high spontaneous differentiation monolayers it was 22.1 ± 7.5%. No differences were observed between monolayers cultured from EOECs harvested from follicular ($n = 6$) versus luteal phase ($n = 4$) oviducts. No significant effect of experiment, mare, or cycle stage on secondary cilia formation was observed ($P > 0.05$). Italic numbers refer to EOEC monolayers considered as high spontaneous differentiated monolayers. Non-italic numbers refer to EOEC monolayers considered as low spontaneous differentiated monolayers.

exception of the percentage of EOECs that developed secondary cilia. We observed that long-term EOEC culture significantly reduced the capacity of the EOECs to form secondary cilia. This difference is pivotal in developing a physiological

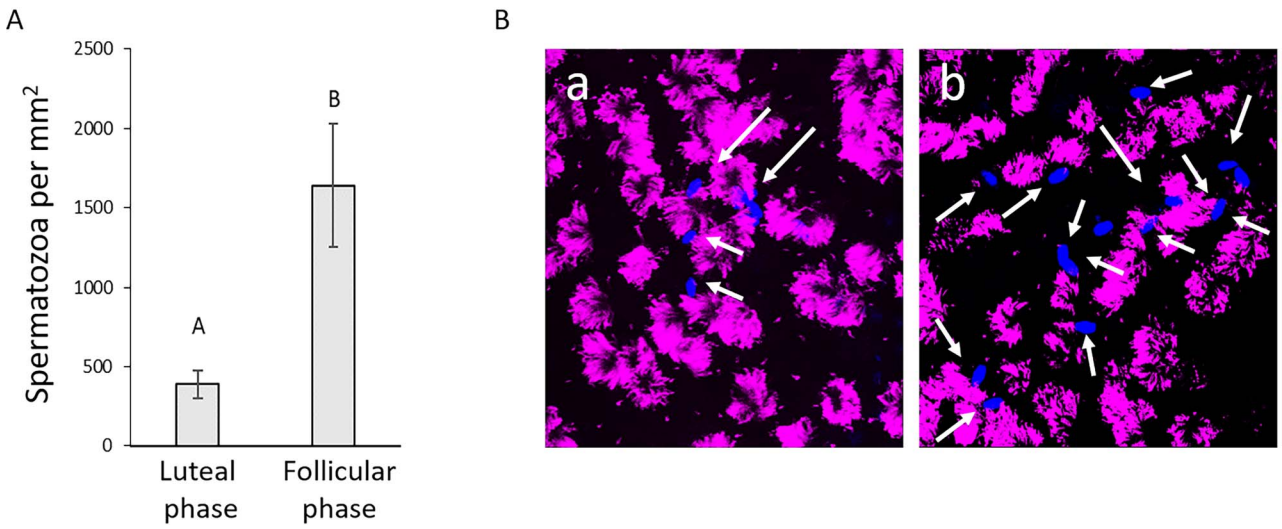

Figure 8. (A) Density of sperm cell binding to re-differentiated EOEC monolayers exposed to cycle stage-dependent hormonal conditions. Different capital letters indicate significant differences in sperm-binding density between luteal and follicular phase stimulated EOEC monolayers ($n = 3$, $P < 0.05$). (B) Representative fluorescent overlay images of bound spermatozoa to EOEC monolayers exposed to (a) luteal and (b) follicular phase hormone conditions. Laser scanning confocal microscopy (630x magnification) was performed to design orthogonal section views from the apical side of the EOECs and the bound spermatozoa. Spermatozoa (DNA in blue: Hoechst 33342), indicated by white arrows, were bound to cilia (purple: acetylated α-tubulin (1:150) detected with goat-anti-rabbit Alexa Fluor 647 (1:100) on the surface of EOEC monolayers.

in vitro oviduct model because the primary and secondary cilia play key roles in monitoring and modulating the extracellular environment, by processing mechanosensory signals, and in generating fluid flow [35]. Moreover, cilia act as secretory organelles and transduce information by releasing small vesicles, termed ectosomes, that play a role in cell–cell communication, intracellular signaling, and cell cycle-related processes [36, 37]. However, cultured EOEC monolayers did demonstrate a number of characteristics required for physiological function. Re-differentiated EOEC monolayers showed significantly higher nuclear progesterone receptor expression when exposed to follicular compared to luteal phase hormone conditions. Additionally, EOEC monolayers exposed to both follicular and luteal hormone regimes bound spermatozoa. Interestingly, sperm-binding density was three times higher in EOEC monolayers exposed to a simulated follicular as compared to a luteal phase hormone environment. A similar difference has been described for bovine sperm–oviduct binding between a few hours pre- and post-ovulation [38].

In other species, such as the pig, mouse, and cow [23], a similar OEC monolayer model was previously developed using the Transwell insert system and showed similar cell morphological features to the in vivo situation. In addition, our group has successfully developed a microfluidic oviduct-on-a-chip that supports bovine fertilization [24]. Interestingly, this oviduct-on-a-chip was able to support similar fertilization rates to standard bovine IVF conditions without addition of the chemical capacitation/fertilization triggers such as heparin, hypotaurine and epinephrine required in the latter. Moreover, the bovine oviduct-on-a-chip facilitated fertilization, while simultaneously reducing the incidence of polyspermy and parthenogenesis [24]. Based on these results, we propose that an improved oviduct model may support equine sperm capacitation and IVF.

Notwithstanding these important findings in the cow, the overall aim of the current study was to optimize techniques for establishing an equine in vitro oviduct epithelial culture in a microfluidic chip. In contrast to previously published work with bovine OECs [25], a direct seeding protocol was unsuccessful with EOECs. The static phase (timespan between cell seeding and start of microfluidic perfusion) was too long for the EOECs. This aspect had an important adverse effect on cell culture in microfluidic chips. In contrast to Transwell inserts that allow cell culture in a relatively large volume of culture medium, establishing EOEC monolayers in the microfluidic chips required a low culture medium volume with a relatively high cell concentration. Overall, EOECs cultured in the microfluidic chips are likely to exhaust nutrients such as glucose from the medium much faster [39, 40], so that the accumulation of cell metabolites such as lactic acid will rise more rapidly [41, 42]. This could exceed the buffering capacity of the medium leading to a drop in the pH and the initiation of cell death [41, 42]. A practical consequence is that the low volume cell culture medium needs to be dynamically refreshed in the chip by microfluidic perfusion starting as soon as possible after cell seeding. The de-differentiation and re-differentiation approach that was pre-tested in Transwell inserts enabled shortening of the static phase (timespan between cell seeding and the start of microfluidic perfusion) to two days. It appeared that de-differentiated EOECs attached much faster to the microporous membrane than differentiated EOECs. After air–liquid interface introduction, this feature allowed the establishment of differentiated oviduct monolayers in microfluidic chips.

The reason why bovine oviduct epithelial vesicles colonized the membrane much faster than EOECs (4 days vs 10 days) may relate to pre-coating of the chips with extracellular matrix components (Matrigel) in the bovine OEC study [25]. Similarly, other Transwell protocols for bovine OEC culture rely on pre-coating the membranes with collagen [23]. Use of attachment factors offers further opportunities to adapt or optimize the EOEC monolayer culture.

In one of the initial experiments in this study, we demonstrated that harvesting of viable EOECs from the ampulla could be achieved efficiently by mechanical scraping or trypsin incubation, techniques that have previously been described for

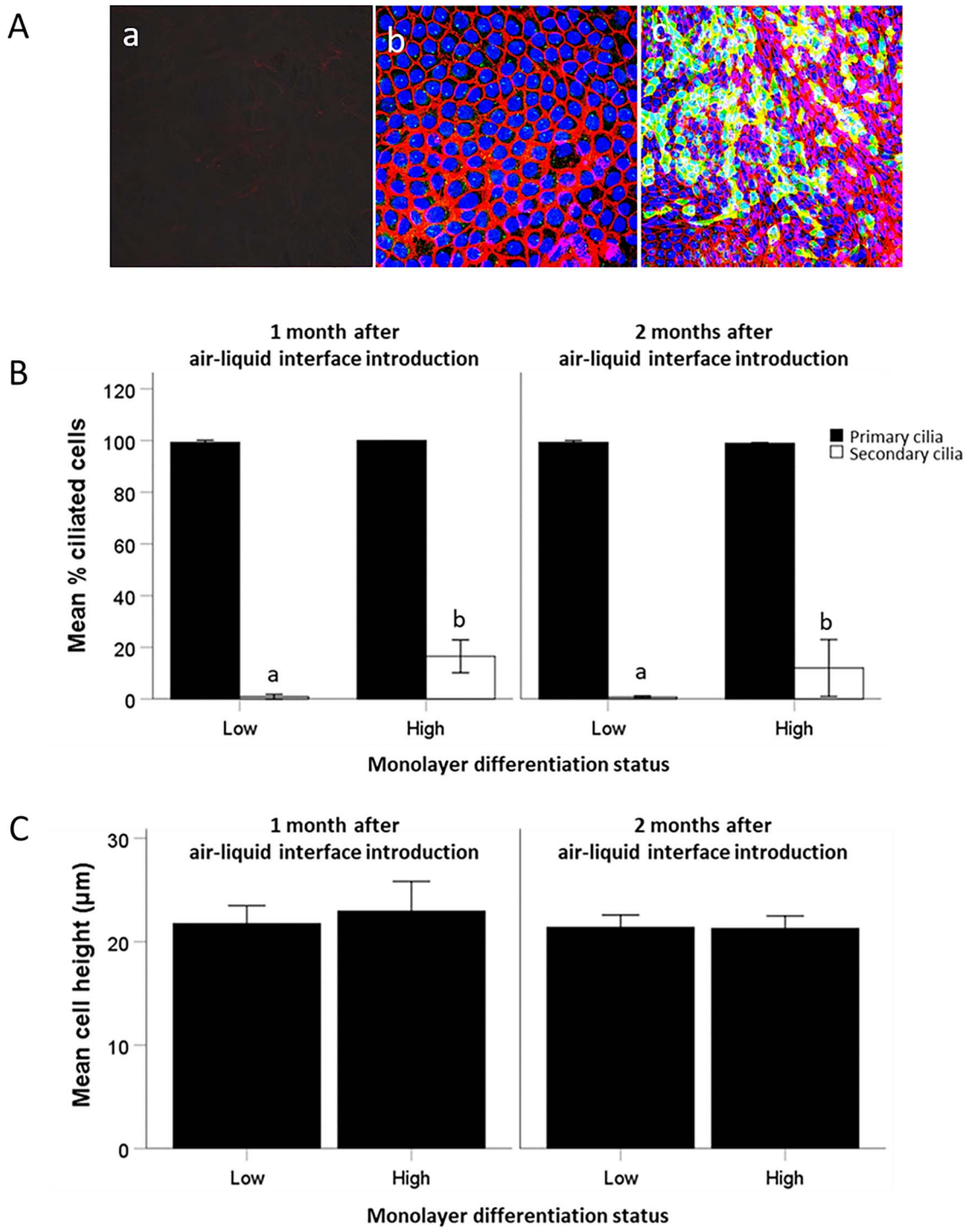

Figure 9. (A) Representative fluorescent images for EOEC monolayers cultured by the direct seeding and re-differentiation protocols in microfluidic chips. (a) Seeding oviduct epithelial vesicles (direct seeding protocol) was not effective for establishing EOEC monolayers. EOECs were not able to attach to the microporous membrane. By contrast, seeding de-differentiated EOECs and subsequently inducing re-differentiation by air–liquid interface introduction supported the formation of confluent monolayers in microfluidic chips (re-differentiation protocol). Similar to culture in Transwell inserts, (b) a monolayer of columnar-polarized EOECs showing primary cilia, but few secondary cilia after introducing an air–liquid interface and (c) exceptional monolayer (only two monolayers in this study) of columnar-polarized EOECs showing primary and secondary cilia (>20%) [green (anti-acetylated α-tubulin antibodies-Alexa Fluor 488 secondary antibody): primary (single green dots at each EOEC) and secondary cilia (many green dots on some EOECs), red (phalloidin conjugated to Alexa Fluor 568): cytoskeleton, blue (Hoechst 33342): nuclei] (original magnification, 400x). (B) The percentage of primary and secondary ciliated EOECs (mean ± s.d.) from low and high spontaneously differentiated oviduct monolayers cultured in microfluidic chips established by the re-differentiation protocol, 1 and 2 months after air liquid interface introduction. Significant differences in the percentage of secondary ciliated EOECs between low and high secondary ciliated monolayers are indicated by different small letters ($P < 0.05$). (C) The cell height (mean ± s.d.) from low and high spontaneously differentiated monolayer EOECs was measured from five different mares for the low spontaneously differentiated monolayers and from two different mares for the high spontaneously differentiated monolayers.

collection of equine oviduct epithelial vesicles [19, 20]. By contrast, efficient harvest of EOECs from the isthmus was very dependent on trypsin digestion. The latter observation may be explained by the much smaller diameter of the isthmus and its more prominent muscular wall compared to the ampulla [43], both of which may compromise physical accessibility. Moreover, the ratio of EOECs to other cells is much lower in the isthmus compared to the ampulla because the surface area of the mucosal folds in the ampulla is much larger than the simple undulating inner surface of the isthmus [43].

Interestingly, the current study showed that de-differentiated EOECs did not lose their capacity to re-differentiate to polarized-columnar cells after introduction of an air–liquid phase. It can thus be hypothesized that de-differentiated EOECs have "transit-amplifying cell" (TAC) characteristics, i.e., a cell population that becomes differentiated after several rounds of cell division [44]. The basic feature of such a "transit" cell population is their capacity to generate many differentiated cells from relatively few precursor cells during development and tissue regeneration [45]. The TAC is considered to be a transitional cell stage between a stem cell and a differentiated cell [46]. Whether the cells harvested from the equine ampulla also contained TACs, or a putative stem cell population, remains an open question. Nevertheless, it should be pointed out that the presence of adult stem cells has been demonstrated in the proximal oviduct [47], suggesting that a stem cell or TAC niche is present in the oviduct.

Culturing EOEC monolayers in submerged conditions supported cell division by mitosis. This process was not, however, indefinite. As time progressed and the monolayers became confluent, progressive formation of large vacuoles was observed, which suggests the onset of senescence in cultured cells by 10–14 days. We therefore consider it important to stimulate the re-differentiation process by air–liquid interface introduction within 10–14 days after the onset of de-differentiation culture. Further research is ongoing to assess the ideal balance between de-differentiation and mitotic capacity, to avoid the onset of cell senescence.

The current study demonstrated that the morphological characteristics of EOEC monolayers cultured by the direct seeding and re-differentiation protocols were very similar to the in vivo situation. A prominent cytoskeleton in confluent monolayers of columnar EOECs was achieved in both hanging Transwell inserts and microfluidic chips. As previously observed for human intestinal cells [48], a tight F-actin network supports monolayer confluency resulting in high TEER values and low tracer flux rates. Furthermore, we could confirm the formation of tight junctions which contribute to the low permeability and high electrical resistance of the cultured EOEC monolayer. Our cut-off value for TEER in intact monolayers in Transwell inserts (462 Ω*cm^2) was similar to the proposed reference range for well-differentiated porcine OEC monolayers (500–1500 Ω*cm^2; [31]). For monolayers cultured in the microfluidic chips, an intact network of F-actin filaments was also observed, and low tracer flux rates were measured. However, TEER measurements remained very low even after 2 months of culture. It must be presumed that the commercial custom-made microfluidic chips allow an electron flux between the apical and the basal compartment outside the membrane where the EOEC monolayer was located. Tracer molecules were clearly not able to pass through this area. This emphasizes the importance of not relying on a singular parameter to characterize monolayer integrity [49, 50].

In addition to the formation of confluent monolayers, the EOECs showed clear signs of an apical-basal polarization, regardless of whether they were obtained by the direct seeding or re-differentiation protocols. A columnar epithelium with a cell height of ~18–25 μm was achieved after re-differentiation of proliferating EOECs. In the basolateral part of the EOEC monolayers, round-oval shaped nuclei were present, while in the apical compartment of >99% of the EOECs a primary cilium was observed. Similar results were reported for porcine [23] and bovine [51] OEC monolayers. In the current and cited studies, air–liquid interface introduction, which reduces shear stress on the apical part of the cell, is the key to inducing cell polarization [28].

Surprisingly, neither protocol resulted in a secondary ciliation rate as high as observed in the in vivo sections. Unfortunately, the mechanism that steers the EOECs to de novo expression of secondary cilia is not yet fully understood. In general, OEC ciliation is thought to be triggered by hormonal cues, e.g., the injection of estrogens promotes ciliogenesis in the OECs of newborn rats [52]. Similarly in the pig, a clear effect of cycle-stage specific hormones, i.e., estradiol and progesterone, on OEC cell height, ciliation rates, and secretory markers has been reported [26]. In the horse, ~60% or 55% of the OECs in tissue sections from the ampulla in the follicular or luteal phase respectively exhibit secondary cilia, and differences between cycle stages were small. Similarly, Desantis et al. [53] reported ciliation rates of ~66%. Inhibition of the notch-signaling pathway could possibly enhance ciliation, since notch inhibition appears to play a key role in secondary cilia formation [54] in organoids derived from human OECs [55].

Previous studies in the pig showed that OECs undergo dramatic functional changes throughout the estrous cycle [56]. In this study, re-differentiated EOEC monolayers exposed to luteal phase hormone conditions demonstrated significantly lower nuclear progesterone receptor expression levels in EOEC monolayers compared to follicular phase hormone conditions. Active downregulation of nuclear progesterone receptor expression by luteal phase hormone conditions in OECs was reported previously by Nelis et al. using an EOEC explant model [33] and Ulbrich et al. using bovine OECs [57]. We hypothesize that the elevated progesterone concentrations of the luteal phase conditions suppress the expression of its own receptor. This has been described previously in guinea-pigs [58, 59], macaques [60], cats [61], and mice [62].

Compared to re-differentiated EOEC monolayers, we observed that oviduct reference tissue exhibited much higher percentages of nuclear progesterone receptor positive EOECs in both luteal and follicular phase oviducts. High nuclear progesterone receptor percentages were also observed previously in luteal phase oviduct reference tissue [11] and oviduct explants [33]. It is possible that a longer period of cyclical hormone exposure, i.e., mimicking several cycles, will modify hormone receptor expression in EOEC monolayers to better mimic the reference tissue phenotype in re-differentiated EOEC monolayers.

Sperm–oviduct binding experiments demonstrated that spermatozoa were mostly bound to cilia present on the EOEC surface. The preference of spermatozoa to bind to cilia has also been observed in vivo in the bovine oviduct [38].

Sperm–binding density was significantly higher when EOECs were exposed to follicular phase hormone concentrations (80 ng/mL E2 and 40 ng/mL P4) compared to luteal phase hormone concentrations (10 ng/mL E2 and 1000 ng/mL P4). This observation suggests a change in membrane molecules at the surface of the EOECs, i.e., the cilia, to facilitate sperm-binding. EOEC monolayers exposed to follicular phase hormones may be a suitable model for studying the molecular nature of sperm–oviduct binding in the horse in future experiments. As suggested above, the question of whether follicular phase hormone conditions positively affect the ciliation rate, and consequently sperm–oviduct binding, remains relevant for future research.

Further studies should focus on unraveling the mechanisms responsible for EOEC phenotype differentiation, with the aim of generating EOEC monolayers in microfluidic chips with a mixed population of secretory and ciliated cells. Moreover, the relationship between EOEC morphology and functionality should be studied in more detail.

Supplementary material

Supplementary material is available at *BIOLRE* online.

Acknowledgements

Images were acquired in the Center for Cellular Imaging (CCI) at the Faculty of Veterinary Medicine Utrecht and we thank Dr R. Wubbolts and E. van 't Veld for their excellent help and technical advice.

Data availability

The data underlying this article will be shared on reasonable request to the corresponding author.

Conflict of interest

The authors have declared that no conflict of interest exists.

References

1. Palmer E, Bezard J, Magistrini M, Duchamp G. In vitro fertilization in the horse. A retrospective study. *J Reprod Fertil Supp* 1991; **44**: 375–384.
2. Bézard J, Magistrini M, Battut I, Duchamp G, Palmer E. In vitro fertilization in the mare. *Recueil De Medecine Veterinaire* 1992; **168**:993–1003.
3. Hinrichs K, Love CC, Brinsko SP, Choi YH, Varner DD. In vitro fertilization of in vitro-matured equine oocytes: effect of maturation medium, duration of maturation, and sperm calcium ionophore treatment, and comparison with rates of fertilization in vivo after oviductal transfer. *Biol Reprod* 2002; **67**:256–262.
4. Choi YH, Okada Y, Hochi S, Braun J, Sato K, Oguri N. In-vitro fertilization rate of horse oocytes with partially removed zonae. *Theriogenology* 1994; **42**:795–802.
5. McPartlin LA, Suarez SS, Czaya CA, Hinrichs K, Bedford-Guaus SJ. Hyperactivation of stallion sperm is required for successful in vitro fertilization of equine oocytes. *Biol Reprod* 2009; **81**:199–206.
6. Dell'Aquila ME, Cho YS, Minoia P, Traina V, Fusco S, Lacalandra GM, Maritato F. Intracytoplasmic sperm injection (ICSI) versus conventional IVF on abottoir-derived and in vitro-matured equine oocytes. *Theriogenology* 1997; **47**:1139–1156.
7. Leemans B, Gadella BM, Stout TAE, Heras S, Smits K, Ferrer-Buitrago M, Claes E, Heindryckx B, De Vos WH, Nelis H, Hoogewijs M, Van Soom A. Procaine induces cytokinesis in horse oocytes via a pH dependent mechanism. *Biol Reprod* 2015; **93**: 1–17.
8. Leemans B, Gadella BM, Stout TAE, De Schauwer C, Nelis H, Hoogewijs M, Van Soom A. Why doesn't conventional IVF work in the horse? The equine oviduct as a microenvironment for capacitation/fertilization. *Reproduction* 2016; **152**:233–245.
9. Leemans B, Stout TAE, De Schauwer C, Heras S, Nelis H, Hoogewijs M, Van Soom A, Gadella BM. Update on mammalian sperm capacitation: how much does the horse differ from other species? *Reproduction* 2019a; **157**:181–197.
10. McCue PM, Fleury JJ, Denniston DJ, Graham JK, Squires EL. Oviductal insemination of mares. *J Reprod Fertil Suppl* 2000; 499–502.
11. Nelis H, Vanden Bussche J, Wojciechowicz B, Franczak A, Vanhaecke L, Leemans B, Cornillie P, Peelman L, Van Soom A, Smits K. Steroids in the equine oviduct: synthesis, local concentrations and receptor expression. *Reprod Fertil Dev* 2015; **28**:1390–1404.
12. Senger PL, Phillip L. *Pathways to Pregnancy and Parturition*. Washington: Current Conceptions, Inc.; 1997: 26–27.
13. Rodriguez-Martinez H. Role of the oviduct in sperm capacitation. *Theriogenology* 2007; **68**:138–146.
14. Coy P, Garcia-Vazquez FA, Visconti PE, Aviles M. Roles of the oviduct in mammalian fertilization. *Reproduction* 2012; **144**: 649–660.
15. Suarez SS. Formation of a reservoir of sperm in the oviduct. *Reprod Domest Anim* 2002; **37**:140–143.
16. Desantis S, Zizza S, Accogli G, Acone F, Rossi R, Resta L. Morphometric and ultrastructural features of the mare oviduct epithelium during oestrus. *Theriogenology* 2011; **75**:671–678.
17. Dobrinski I, Jacob JR, Tennant BC, Ball BA. Generation of an equine oviductal epithelial cell line for the study of sperm-oviduct interactions. *Theriogenology* 1999; **52**:875–885.
18. Thomas PG, Ignotz GG, Ball BA, Miller PG, Brinsko SP, Currie B. Isolation, culture, and characterization of equine oviduct epithelial cells in vitro. *Mol Reprod Dev* 1995; **41**:468–478.
19. Nelis H, D'Herde K, Goossens K, Vandenberghe L, Leemans B, Forier K, Smits K, Braeckmans K, Peelman L, Van Soom A. Equine oviduct explant culture: a basic model to decipher embryo-maternal communication. *Reprod Fertil Dev* 2014; **26**: 954–966.
20. Leemans B, Gadella BM, Sostaric E, Nelis H, Stout TAE, Hoogewijs M, Van Soom A. Oviduct binding and elevated environmental pH induce protein tyrosine phosphorylation in stallion spermatozoa. *Biol Reprod* 2014; **91**:1–12.
21. Leemans B, Stout TAE, Van Soom A, Gadella BM. pH-dependent effects of procaine on equine gamete activation. *Biol Reprod* 2019b; **101**:1056–1074.
22. Leemans B, Gadella BM, Stout TAE, Nelis H, Hoogewijs M, Van Soom A. An alkaline follicular fluid fraction induces capacitation and limited release of oviduct epithelium-bound stallion sperm. *Reproduction* 2015; **150**:193–208.
23. Chen S, Palma-Vera SE, Langhammer M, Galuska SP, Braun BC, Krause E, Lucas-Hahn A, Schoen J. An air-liquid interphase approach for modeling the early embryo-maternal contact zone. *Sci Rep* 2017; **7**:42298.
24. Ferraz MA, Henning HH, Costa PF, Malda J, Melchels FP, Wubbolts R, Stout TAE, Vos PL, Gadella BM. Improved bovine embryo production in an oviduct-on-a-chip system: prevention of polyspermic fertilization and parthenogenic activation. *Lab Chip* 2017; **17**:905–916.
25. Ferraz MA, Suk Rho H, Hemerich D, Henning HH, van Tol H, Hölker M, Besenfelder U, Mokry M, Vos PL, Stout TAE, Le Gac S, Gadella BM. An oviduct-on-a-chip provides an enhanced in vitro environment for zygote genome reprogramming. *Nat Commun* 2018; **9**:1–14.
26. Chen S, Einspanier R, Schoen J. In vitro mimicking of estrous cycle stages in porcine oviduct epithelium cells: estradiol and progesterone regulate differentiation, gene expression, and cellular function. *Biol Reprod* 2013; **89**:1–12.

27. Chen S, Palma-Vera SE, Kempisty B, Rucinski M, Vernunft A, Schoen J. In vitro mimicking of estrous cycle stages: dissecting the impact of estradiol and progesterone on oviduct epithelium. *Endocrinology* 2018; **159**:3421–3432.
28. Miessen K, Sharbati S, Einspanier R, Schoen J. Modelling the porcine oviduct epithelium: a polarized in vitro system suitable for long-term cultivation. *Theriogenology* 2011; **76**:900–910.
29. Ellington JE, Varner DD, Burghardt RC, Meyers-Wallen VN, Barhoumi R, Brinsko SP, Ball BA. Cell-to-cell communication of equine uterine tube (oviduct) cells as determined by anchored cell analysis in culture. *Anim Reprod Sci* 1993; **30**:313–324.
30. Schindelin J, Arganda-Carreras I, Frise E, Kaynig V, Longair M, Pietzsch T, Preibisch S, Rueden C, Saalfeld S, Schmid B, Tinevez J, White DJ *et al*. Fiji: an open-source platform for biological-image analysis. *Nat Methods* 2012; **9**:676–682.
31. Chen S, Einspanier R, Schoen J. Transepithelial electrical resistance (TEER): a functional parameter to monitor the quality of oviduct epithelial cells cultured on filter supports. *Histochem Cell Biol* 2015; **144**:509–515.
32. Nagaoka K, Nambo Y, Nagamine N, Nagata S, Tanaka Y, Shinbo H, Tsunoda N, Taniyama H, Watanabe G, Groome NP, Taya K. A selective increase in circulating inhibin and inhibin pro-αC at the time of ovulation in the mare. *Am J Physiol* 1999; **277**:870–875.
33. Nelis H, Wojciechowicz B, Franczak A, Leemans B, D'Herde K, Goossens K, Cornillie P, Peelman L, Van Soom A, Smits K. Steroids affect gene expression, ciliary activity, glucose uptake, progesterone receptor expression and immunoreactive steroidogenic protein expression in equine oviduct explants in vitro. *Reprod Fertil Dev* 2015; **28**:1926–1944.
34. Brogan PT, Beitsma M, Henning H, Gadella BM, Stout TAE. Liquid storage of equine semen: assessing the effect of d-penicillamine on longevity of ejaculated and epididymal stallion sperm. *Anim Reprod Sci* 2015; **159**:155–162.
35. Mitchell DR. Evolution of cilia. *Cold Spring Harb Perspect Biol* 2017; **9**:a028290.
36. Mirvis M, Stearns T, James NW. Cilium structure, assembly, and disassembly regulated by the cytoskeleton. *Biochem J* 2018; **475**: 2329–2353.
37. Kumar D, Richard EM, Betty AE, Stephen MK. Ciliary and cytoskeletal functions of an ancient monooxygenase essential for bioactive amidated peptide synthesis. *Cell Mol Life Sci* 2019; **76**: 2329–2348.
38. Sostaric E, Dieleman SJ, van de Lest CH, Colenbrander B, Vos PL, Garcia-Gil N, Gadella BM. Sperm binding properties and secretory activity of the bovine oviduct immediately before and after ovulation. *Mol Reprod Dev* 2008; **75**:60–74.
39. Heywood HK, Bader DL, Lee DA. Glucose concentration and medium volume influence cell viability and glycosaminoglycan synthesis in chondrocyte-seeded alginate constructs. *Tissue Eng* 2006a; **12**:3487–3496.
40. Heywood HK, Bader DL, Lee DA. Rate of oxygen consumption by isolated articular chondrocytes is sensitive to medium glucose concentration. *J Cell Physiol* 2006b; **206**:402–410.
41. Bayrock DP, Ingledew WM. Inhibition of yeast by lactic acid bacteria in continuous culture: nutrient depletion and/or acid toxicity? *J Ind Microbiol Biotechnol* 2004; **31**:362–368.
42. Leroy F, De Vuyst L. Growth of the bacteriocin-producing *Lactobacillus sakei* strain CTC 494 in MRS broth is strongly reduced due to nutrient exhaustion: a nutrient depletion model for the growth of lactic acid bacteria. *Appl Environ Microbiol* 2001; **67**: 4407–4413.
43. McKinnon AO, Squires EL, Vaala WE, Varner DD. *Equine Reproduction*, 2nd ed. John Wiley & Sons; 2011.
44. Hsu YC, Li L, Fuchs E. Transit-amplifying cells orchestrate stem cell activity and tissue regeneration. *Cell* 2014; **157**:935–949.
45. Loeffler M, Bratke T, Paulus U, Li YQ, Potten CS. Clonality and life cycles of intestinal crypts explained by a state dependent stochastic model of epithelial stem cell organization. *J Theor Biol* 1997; **186**: 41–54.
46. Rangel-Huerta E, Maldonado E. Transit-amplifying cells in the fast lane from stem cells towards differentiation. *Stem Cells Int* 2017; **2017**:1–10.
47. Ng A, Tan S, Singh G, Rizk P, Swathi Y, Tan TZ, Yun-Ju Huang R, Leushacke M, Barker N. Lgr5 marks stem/progenitor cells in ovary and tubal epithelia. *Nat Cell Biol* 2014; **16**:745–757.
48. Karwad MA, Macpherson T, Wang B, Theophilidou E, Sarmad S, Barrett DA, Larvin M, Wright KL, Lund JN, O'Sullivan SE. Oleoylethanolamine and palmitoylethanolamine modulate intestinal permeability in vitro via TRPV1 and PPARα. *FASEB J* 2017; **31**:469–481.
49. Benson K, Cramer S, Galla HJ. Impedance-based cell monitoring: barrier properties and beyond. *Fluids Barriers CNS* 2013; **10**:5–16.
50. Bischoff I, Hornburger MC, Mayer BA, Beyerle A, Wegener J, Fürst R. Pitfalls in assessing microvascular endothelial barrier function: impedance-based devices versus the classic macromolecular tracer assay. *Sci Rep* 2016; **6**:23671.
51. Ferraz MA, Henning HH, Stout TAE, Vos PL, Gadella BM. Designing 3-dimensional in vitro oviduct culture systems to study mammalian fertilization and embryo production. *Ann Biomed Eng* 2016; **45**:1731–1744.
52. Okada A, Ohta Y, Brody SL, Watanabe H, Krust A, Chambon P, Iguchi T. Role of foxj1 and estrogen receptor alpha in ciliated epithelial cell differentiation of the neonatal oviduct. *J Mol endocrinol* 2004; **32**:615–625.
53. Desantis S, Ventriglia G, Zubani D, Corriero A, Deflorio M, Acone F, Palmieri G, De Metrio G. Differential lectin binding patterns in the oviductal ampulla of the horse during oestrus. *Eur J Histochem* 2005; **49**:139–149.
54. Choksi SP, Lauter G, Swoboda P, Roy S. Switching on cilia: transcriptional networks regulating ciliogenesis. *Development* 2014; **14**:1427–1441.
55. Kessler M, Hoffmann K, Brinkmann V, Thieck O, Jackisch S, Toelle B, Berger H, Mollenkopf HJ, Mangler M, Sehouli J. The notch and Wnt pathways regulate stemness and differentiation in human fallopian tube organoids. *Nat Commun* 2015; **6**:1–11.
56. Abe H, Hoshi H. Regional and cyclic variations in the ultrastructural features of secretory cells in the oviductal epithelium of the Chinese Meishan pig. *Reprod Domest Anim* 2007; **42**: 292–298.
57. Ulbrich SE, Kettler A, Einspanier R. Expression and localization of estrogen receptor alpha, estrogen receptor beta and progesterone receptor in the bovine oviduct in vivo and in vitro. *J Steroid Biochem Mol Biol* 2003; **84**:279–289.
58. Vu Hai MT, Warembourg M, Milgrom E. Hormonal control of progesterone receptors. *Ann N Y Acad Sci* 1977; **286**:199–209.
59. Alkhalaf M, Propper AY, Chaminadas G, Adessi GL. Ultrastructural changes in Guinea pig endometrial cells during the estrous cycle. *J Morphol* 1992; **214**:83–96.
60. West NB, Brenner RM. Progesterone-mediated suppression of estradiol receptors in cynomolgus macaque cervix, endometrium and oviduct during sequential estradiol-progesterone treatment. *J Steroid Biochem* 1985; **22**:29–37.
61. West NB, Verhage HG, Brenner RM. Changes in nuclear estradiol receptor and cell structure during estrous cycles and pregnancy in the oviduct and uterus of cats. *Biol Reprod* 1977; **17**: 138–143.
62. Tibbetts TA, Mendoza-Meneses M, O'Malley BW, Conneely OM. Mutual and intercompartmental regulation of estrogen receptor and progesterone receptor expression in the mouse uterus. *Biol Reprod* 1998; **59**:1143–1152.